





## Conditions for separability in multiqubit systems with an accelerating qubit using a conditional entropy

Harsha Miriam Reji , Hemant S. Hegde , and R. Prabhu 

*Department of Physics, Indian Institute of Technology Dharwad, Dharwad, Karnataka 580007, India*

 (Received 12 April 2024; revised 4 August 2024; accepted 20 August 2024; published 4 September 2024)

We study the separability in multiqubit pure and mixed Greenberger-Horne-Zeilinger (GHZ) and  $W$  states with an accelerating qubit using the Abe-Rajagopal (AR)  $q$ -conditional entropy. We observe that the pure multiqubit GHZ and  $W$  states in the inertial-noninertial bipartition with one of their qubits accelerated will remain nonseparable irrespective of the qubit's acceleration. In these systems, we capture the variation of their nonseparability with respect to the acceleration of the qubit and the AR  $q$ -conditional entropy parameter  $q$ . However, in the corresponding multiqubit mixed states obtained by introducing a global noise to the above pure states, we could get stronger conditions on their separability in the inertial-noninertial bipartition, in terms of the acceleration of the qubit, the noise parameter, and the number of qubits in the system, in the asymptotic limit of the parameter  $q$ . These conditions obtained from the AR  $q$ -conditional entropy serve as necessary conditions for separability in such multiqubit states with a relativistic qubit.

DOI: [10.1103/PhysRevA.110.032403](https://doi.org/10.1103/PhysRevA.110.032403)

### I. INTRODUCTION

A vast majority of quantum information tasks, such as quantum teleportation [1–3], quantum dense coding [4], and quantum key distribution, [5,6] rely on quantum correlations present in quantum systems [7,8]. Recently, it has been established that the quantum correlations present in quantum systems vary when their subsystems are relativistically accelerated [9–11]. The characterization of quantum correlations and quantum information protocols in quantum systems with accelerated subsystems has led to the emergence of relativistic quantum information. Currently, relativistic quantum information involves studies that characterize and quantify entanglement in bosonic [9,12–16] and fermionic [17–27] modes when their subsystems are in noninertial frames, entanglement near black holes [28–33], entanglement in the expanding universe [34–38], relativistic quantum metrology [39–42], quantum discord in relativistic states [11,43], relativistic quantum teleportation [44–46], the relativistic quantum speed limit [47–49], etc.

There has been considerable interest in using entropic measures to characterize separability in composite quantum systems in the inertial frame [50–55]. For pure states, the separability criteria using von Neumann conditional entropy suggest that nonseparable quantum systems are more disordered locally than globally [56]. In the case of mixed states, the generalized entropic measures have been introduced to better understand and explore valuable quantum information properties [57–61]. The two prominent families of these generalized entropies are the Tsallis  $q$  entropy [62,63] and  $\alpha$ -Rényi entropy [64], which reduce to the von Neumann entropy as  $q$  approaches 1. Their positive values help distinguish between global and local disorder in mixed states.

To study the separability of quantum states with an accelerating qubit, we use a generalized form of conditional entropy

called the Abe-Rajagopal (AR)  $q$ -conditional entropy, derived from the Tsallis  $q$  entropy [65,66]. The AR  $q$ -conditional entropy depends on the global versus local spectra of the composite quantum system and it assumes a negative value for nonseparable states. However, AR  $q$ -conditional entropic characterization is not always a necessary and sufficient condition for separability. Notwithstanding, it can offer stricter limitations on separability compared to traditional methods like the von Neumann conditional entropy [67]. Further, a negative AR  $q$ -conditional entropy indicates that the composite quantum state is distillable, as it implies a violation of the reduction criterion [68]. Previously, this conditional entropy was applied to study the separability in a single parameter family of mixed multiqubit states [67] and Gaussian states [69]. Here we use the AR  $q$ -conditional entropy to characterize the nonseparability of several multipartite quantum states in the inertial-noninertial bipartition.

We initially consider a generalized pure two-qubit Greenberger-Horne-Zeilinger (GHZ) state with one of its qubits under acceleration and characterize its nonseparability in the inertial-noninertial bipartition with respect to system parameters, acceleration of the qubit, and the parameter  $q$ . Since the characterization of nonseparability using the AR  $q$ -conditional entropy uses all the eigenvalues of the state and corresponding subsystem, we introduce an eigenvalue truncation procedure to handle the infinite eigenvalues in such systems numerically. Subsequently, we will extend our nonseparability characterization to the pure multiqubit GHZ and  $W$  states. Later, we will explore the nonseparability in mixed states generated by mixing a global noise with the above pure multiqubit GHZ and  $W$  states. Since these accelerated mixed states and their subsystems do not possess a block structure to obtain their eigenvalues analytically, we introduce a density-matrix truncation procedure to evaluate the AR  $q$ -conditional entropy numerically. We derive conditions for

separability in these mixed multiqubit states, which depend on their mixing parameter, the acceleration of the qubit, and the number of qubits in the multiqubit state in the asymptotic limit of the parameter  $q$ . The findings on the nonseparability conditions for the mixed multiqubit states reveal significant insights when compared with the entanglement measure of logarithmic negativity. The AR  $q$ -conditional entropy imposes a more stringent condition for nonseparability than logarithmic negativity in single-qubit-accelerated multiqubit mixed states. However, both measures are equivalent for single-qubit-accelerated pure multiqubit states, a crucial observation in the study of nonseparability measures.

This paper is structured as follows. In Sec. II we describe the bosonic quantum system in a noninertial frame. In Sec. III we succinctly describe the quantification of nonseparability using the AR  $q$ -conditional entropy in an arbitrary bipartite quantum system. In Sec. IV the nonseparability of pure multiqubit GHZ and  $W$  states with one of its qubits being accelerated using the AR  $q$ -conditional entropy is characterized with respect to acceleration, the parameter  $q$ , and the number of qubits in the system. In Sec. V we give a detailed account of obtaining the nonseparability of mixed multiqubit states obtained by adding a global noise to the pure states considered in Sec. IV. Also, the strongest condition for separability for these states is identified in the asymptotic limit of  $q$ . A comparison of separability criteria obtained from AR  $q$ -conditional entropy and logarithmic negativity is presented in Sec. VI. In Sec. VII we present a summary and discuss prospects for future work.

## II. RELATIVISTICALLY ACCELERATED QUANTUM STATE

Consider an arbitrary two-qubit state  $\rho_{AB}$  in an inertial frame shared between the two observers Alice and Bob. When Bob undergoes a relativistic acceleration, henceforth called Rob (relativistically accelerated Bob), his qubit experiences a different space-time around it. While Minkowski coordinates are commonly employed to depict the qubits in the inertial frames, they are unsuitable for describing the motion of an accelerated qubit. In noninertial frames, Rindler coordinates are more appropriate for describing the accelerating qubits. The schematic representation of the Rindler space-time is provided in Fig. 1. The Rindler space-time is divided into two distinct regions, region I (pink shade) and region II (green shade), containing all points mapped from the Minkowski coordinates. Using Bogoliubov transformations, the vacuum state and the single excited state in Minkowski coordinates will individually take the form of a two-mode squeezed state in Rindler space-time [9,44], i.e.,

$$|0_k\rangle_M = \frac{1}{\cosh r} \sum_{n=0}^{\infty} \tanh^n r |n_k\rangle_I \otimes |n_k\rangle_{II} \quad (1)$$

and

$$|1_k\rangle_M = \frac{1}{\cosh^2 r} \sum_{n=0}^{\infty} \tanh^n r \sqrt{n+1} |(n+1)_k\rangle_I \otimes |n_k\rangle_{II}, \quad (2)$$

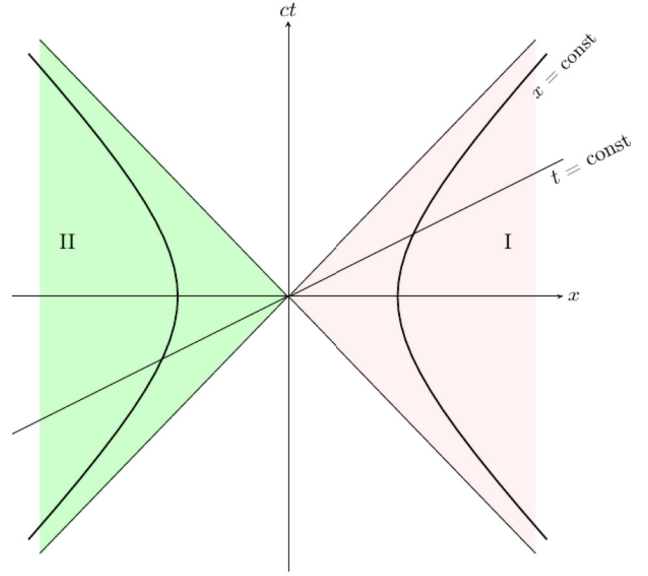


FIG. 1. Schematic representation of Rindler space-time [44], where  $t$  is the proper time, and  $x = \text{const}$  is the trajectory of a qubit with constant acceleration. The pink-shaded region to the right of the vertical axis denotes region I and the green-shaded region to the left of the vertical axis denotes region II of Rindler space-time.

respectively. Here  $|n_k\rangle_I$  and  $|n_k\rangle_{II}$  are the number states of the  $k$ th mode in regions I and II of the Rindler space-time, respectively. The right-hand sides of Eqs. (1) and (2) correspond to a two-mode squeezed state, with the squeezing parameter  $r$  being related to the acceleration  $a$  of Rob's qubit as  $\cosh r = (1 - e^{-2\pi|k|c/a})^{-1/2}$ . Here  $c$  is the speed of light in a vacuum.

A composite state shared between Alice and Bob in the inertial frame  $\rho_{AB}$  transforms as  $\rho_{AR_I R_{II}}$  when Bob's qubit is accelerated. However, the qubit moving in one of the regions of the Rindler space-time cannot travel into the other region as they are causally disconnected. Without any loss of generality, one can trace out the modes of region II ( $R_{II}$ ) of the accelerating qubit. Since a part of the accelerating state has been traced out, the final state between Alice  $A$  and Rob's modes in the region I ( $R_I$ ) is a mixed state and is in the basis  $\{|0\rangle_M |n\rangle_I, |0\rangle_M |n+1\rangle_I, |1\rangle_M |n\rangle_I, |1\rangle_M |n+1\rangle_I\}$  with  $n$  going from zero to  $\infty$ . Henceforth, we will drop all the subscripts  $M$  and  $I$  in the inertial basis  $\{|0\rangle, |1\rangle\}$  as well as accelerating qubit's basis  $\{|n\rangle, |n+1\rangle\}$  and denote the resultant mixed state of Alice and Rob's mode in the region I by  $\rho_{AR}$  and Rob's subsystem by  $\rho_R$ .

## III. ABE-RAJAGOPAL $q$ -CONDITIONAL ENTROPY

The Tsallis  $q$  entropy gives a nonextensive generalization of Shannon entropy [62,63], which is always positive and adheres to the nonadditivity relationship for the bipartite state  $\rho_{XY}$ , i.e.,  $S_q^T(\rho_{XY}) = S_q^T(\rho_X) + S_q^T(\rho_Y) + (1-q)S_q^T(\rho_X)S_q^T(\rho_Y)$ , where  $S_q^T(\rho)$  is given by

$$S_q^T(\rho) = \frac{\text{Tr}(\rho^q) - 1}{1 - q}. \quad (3)$$

Here  $\text{Tr}$  denotes the trace of the corresponding density matrix. However, this nonadditivity condition is violated by the state  $\rho_{XY}$  when subsystems  $X$  and  $Y$  exhibit long-range interactions, such as entanglement, which persists even when they are spatially separated by a long distance. To address this, a conditional form of Tsallis  $q$  entropy was introduced by Abe and Rajagopal [65], called the Abe-Rajagopal  $q$ -conditional entropy, and is defined as

$$S_q(X|Y) = \frac{S_q^T(\rho_{XY}) - S_q^T(\rho_Y)}{1 + (1 - q)S_q^T(\rho_Y)}, \quad (4)$$

where  $S_q^T(\rho_{XY})$  and  $S_q^T(\rho_Y)$  denote the Tsallis  $q$  entropies associated with the composite system  $\rho_{XY}$  and its subsystem  $\rho_Y$ . The computable form of this conditional entropy for any  $X$ - $Y$  bipartition in a multiqubit state can be obtained by plugging Eq. (3) in Eq. (4) and is given by

$$\begin{aligned} S_q(X|Y) &= \frac{1}{q-1} \left( 1 - \frac{\text{Tr}(\rho_{XY}^q)}{\text{Tr}[\rho_Y^q]} \right) \\ &= \frac{1}{q-1} \left( 1 - \frac{\sum_n \lambda_n^q(\rho_{XY})}{\sum_m \lambda_m^q(\rho_Y)} \right), \end{aligned} \quad (5)$$

where  $\lambda_n$  and  $\lambda_m$  are the eigenvalues of the whole system  $\rho_{XY}$  and one of its subsystem  $\rho_Y$ , respectively. This conditional entropy adheres to the nonadditivity relation:  $S_q^T(\rho_{XY}) = S_q(X|Y) + S_q^T(\rho_Y) + (1 - q)S_q(X|Y)S_q^T(\rho_Y)$ . The AR  $q$ -conditional entropy yields negative values for the nonseparable states and hence the positivity of the AR  $q$ -conditional entropy forms a criterion for capturing the separability in bipartite states. From here on, we represent  $S_q(X|Y)$  and  $\mathcal{S}_q(X|Y)$  as the AR  $q$ -conditional entropy for pure  $\rho_{XY}$  and mixed  $\rho_{XY}$  states with one of their qubit being accelerated, respectively.

#### IV. PURE MULTIQUBIT STATES WITH AN ACCELERATING QUBIT

In this section we consider pure multiqubit GHZ and  $W$  states with an accelerated qubit and characterize their nonseparability in the inertial-noninertial bipartition using the AR  $q$ -conditional entropy given in Eq. (5) with respect to their system parameters, the parameter  $q$ , and acceleration of the qubit in the noninertial frame.

##### A. Pure multiqubit GHZ states

###### 1. Generalized pure two-qubit GHZ state

A generalized pure two-qubit GHZ state shared between Alice and Bob in the inertial frame is given by

$$|\text{GHZ}_2\rangle = \cos\theta |00\rangle + \sin\theta |11\rangle, \quad \cos^2\theta + \sin^2\theta = 1, \quad (6)$$

which belongs to the Hilbert space  $H_A \otimes H_B$ . Let Bob's qubit be relativistically accelerated with respect to Alice's qubit, and the resulting composite state  $\rho_{AR_1R_B}^{\text{GHZ}_2}$  is obtained by using the transformations of  $|0\rangle$  and  $|1\rangle$  from Minkowski space-time to Rindler space-time as given in Eqs. (1) and (2). We now obtain the marginal mixed density matrix between Alice and Rob's modes in region I, by following the recipe given in

Sec. II, as

$$\begin{aligned} \rho_{AR}^{\text{GHZ}_2} &= \frac{1}{\cosh^2 r} \sum_n \tanh^{2n} r \left( \cos^2\theta |0n\rangle \langle 0n| + \frac{n+1}{\cosh^2 r} \right. \\ &\quad \times \sin^2\theta |1n+1\rangle \langle 1n+1| + \frac{\sqrt{n+1}}{\cosh r} \\ &\quad \left. \times \cos\theta \sin\theta (|1n+1\rangle \langle 0n| + |0n\rangle \langle 1n+1|) \right). \end{aligned} \quad (7)$$

The structure of this density matrix contains  $2 \times 2$  blocks along the diagonal, with the remaining off-diagonal elements being zero, and is given by

$$\rho_{AR}^{\text{GHZ}_2} = \frac{1}{\cosh^2 r} \begin{pmatrix} 0 & & & & & \\ & \Delta_0 & & & & \\ & & \Delta_1 & & & \\ & & & \ddots & & \\ & & & & \Delta_n & \\ & & & & & \ddots \end{pmatrix}, \quad (8)$$

where

$$\Delta_n(\rho_{AR}^{\text{GHZ}_2}) = \tanh^{2n} r \begin{pmatrix} \cos^2\theta & \alpha_n \cos\theta \sin\theta \\ \alpha_n \cos\theta \sin\theta & \alpha_n^2 \sin^2\theta \end{pmatrix}, \quad (9)$$

with  $\alpha_n = \frac{\sqrt{n+1}}{\cosh r}$ . The eigenvalues of this  $n$ th block of the state  $\rho_{AR}^{\text{GHZ}_2}$  are 0 and

$$\Lambda_n = \frac{\tanh^{2n} r}{\cosh^2 r} \left( \cos^2\theta + \frac{n+1}{\cosh^2 r} \sin^2\theta \right). \quad (10)$$

Therefore,  $\text{Tr}(\rho_{AR}^{\text{GHZ}_2}) = \sum_{n=0}^{\infty} \Lambda_n = 1$ .

The marginal density matrix  $\rho_R^{\text{GHZ}_2}$  corresponding to the modes of Rob in region I of Rindler space-time is computed by tracing out Alice's subsystem  $A$ , i.e.,  $\rho_R^{\text{GHZ}_2} = \text{Tr}_A(\rho_{AR}^{\text{GHZ}_2})$ , and is given by

$$\begin{aligned} \rho_R^{\text{GHZ}_2} &= \frac{1}{\cosh^2 r} \sum_{m=0}^{\infty} \tanh^{2m} r \left( \cos^2\theta |m\rangle \langle m| \right. \\ &\quad \left. + \frac{m+1}{\cosh^2 r} \sin^2\theta |m+1\rangle \langle m+1| \right). \end{aligned} \quad (11)$$

This is an infinite-dimensional diagonal matrix whose  $m$ th eigenvalue is given by

$$\Lambda_m = \frac{\tanh^{2m} r}{\cosh^2 r} \left( \cos^2\theta + \frac{m}{\sinh^2 r} \sin^2\theta \right). \quad (12)$$

Here  $\text{Tr}(\rho_R^{\text{GHZ}_2}) = \sum_{m=0}^{\infty} \Lambda_m = 1$ .

To characterize the nonseparability of the state  $\rho_{AR}^{\text{GHZ}_2}$  given in Eq. (7), we substitute the eigenvalues  $\Lambda_n$  of  $\rho_{AR}^{\text{GHZ}_2}$  [see Eq. (10)] and  $\Lambda_m$  of  $\rho_R^{\text{GHZ}_2}$  [see Eq. (12)] in the AR  $q$ -conditional entropy given in Eq. (5) to obtain

$$\begin{aligned} S_q^{\text{GHZ}_2}(A|R) &= \frac{1}{q-1} \left( 1 - \frac{\sum_{n=0}^{\infty} \left[ \tanh^{2n} r \left( \cos^2\theta + \sin^2\theta \frac{n+1}{\cosh^2 r} \right) \right]^q}{\sum_{m=0}^{\infty} \left[ \tanh^{2m} r \left( \cos^2\theta + \sin^2\theta \frac{m}{\sinh^2 r} \right) \right]^q} \right). \end{aligned} \quad (13)$$

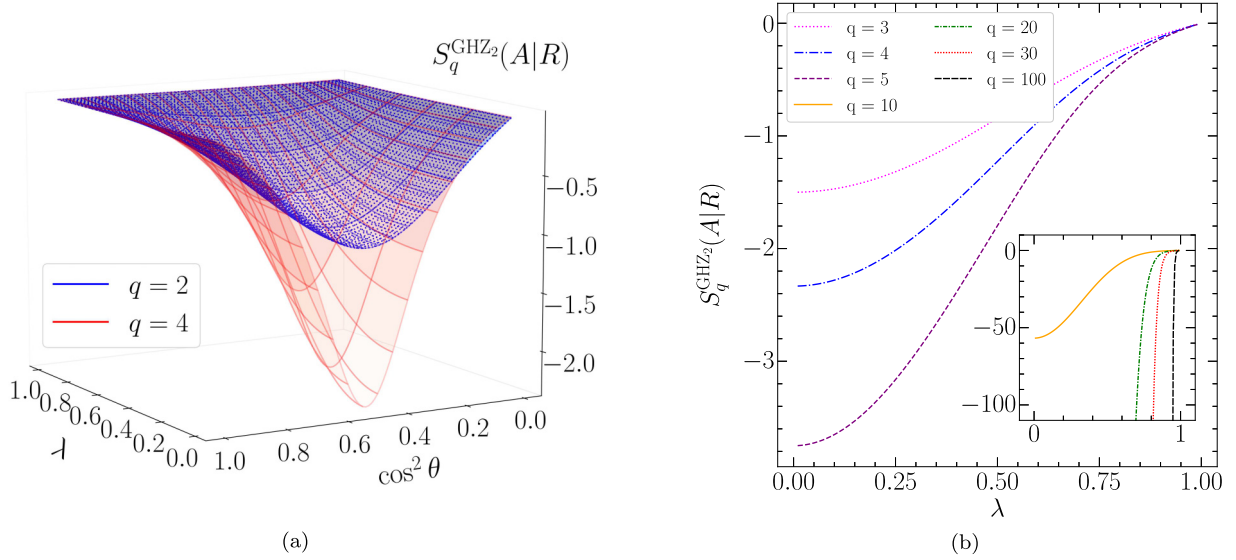


FIG. 2. (a) Variation of the Abe-Rajagopal  $q$ -conditional entropy as a nonseparability feature of a single-qubit-accelerated generalized pure two-qubit GHZ state as a function of  $\cos^2 \theta$  and  $\lambda$  for the parameter  $q = 2$  and 4. The upper blue solid mesh corresponds to  $q = 2$  and the lower red solid mesh corresponds to  $q = 4$ . The  $S_q^{\text{GHZ}_2}(A|R)$  is negative everywhere, implying that the state is nonseparable. For this plot, we have chosen 100 values each of  $\cos^2 \theta$  and  $\lambda$  to create the surface, and the meshes are drawn for representation purposes. (b) Variation of the AR  $q$ -conditional entropy of the pure two-qubit GHZ state with  $\theta = \pi/4$  as a function of  $\lambda$  for different values of the parameter  $q$ .

The negative values of this AR  $q$ -conditional entropy  $S_q^{\text{GHZ}_2}(A|R)$  characterize the nonseparability between Alice's qubit and Rob's mode in region I of the Rindler space-time. As the above expression contains summations running up to infinity, we have to evaluate  $S_q^{\text{GHZ}_2}(A|R)$  numerically to study its behaviors with respect to the state parameter, the acceleration parameter  $r$ , and the parameter  $q$ .

*Eigenvalue truncation procedure.* To numerically compute this conditional entropy, we make use of the fact that the sum of the nonzero eigenvalues of  $\rho_{AR}^{\text{GHZ}_2}$  and  $\rho_R^{\text{GHZ}_2}$  tends to 1 as their respective numbers of eigenvalues  $n$  and  $m$  approach infinity. We achieve this numerically by fixing a large value of  $n \simeq k$  and  $m \simeq k$  such that the sum of  $k$  eigenvalues approaches 1. By inspection, we find that this is satisfied for both states  $\rho_{AR}^{\text{GHZ}_2}$  and  $\rho_R^{\text{GHZ}_2}$  when  $k \approx 10^4$ . Now, using these  $k$  eigenvalues of  $\rho_{AR}^{\text{GHZ}_2}$  and  $\rho_R^{\text{GHZ}_2}$ , we numerically compute the AR  $q$ -conditional entropy given in Eq. (13) and characterize the nonseparability of the state in Eq. (7) with respect to the parameter  $q$ , the state parameter  $\theta$ , and Rob's acceleration  $r$ .

We now introduce the modified acceleration parameter  $\lambda = \tanh r$ , which carries all the characteristics of Rob's acceleration  $r$ , i.e., we use  $\lambda \in (0, 1)$  instead of  $r \in (0, \infty)$ . For simplicity, we call  $\lambda$  Rob's acceleration. The AR  $q$ -conditional entropy for the state given in Eq. (7) is then plotted as a function of its state parameter  $\theta$  and acceleration of Rob's  $\lambda$  in Fig. 2(a) for  $q = 2$  (upper blue surface) and 4 (lower red surface). We observe that  $S_q^{\text{GHZ}_2}(A|R)$  always remains less than zero, implying that the state remains nonseparable for any values of  $\lambda$  and  $\theta$ . A higher negative value of the AR  $q$ -conditional entropy implies higher nonseparability; however, this does not necessarily imply a higher entanglement in mixed states. Note that  $S_q^{\text{GHZ}_2}(A|R)$  attains maximum

nonseparability at  $\theta = \pi/4$ , irrespective of the parameter  $q$ . When  $\theta = \pi/4$ , Eq. (6) corresponds to a maximally entangled two-qubit Bell state in an inertial frame. Hence, in Fig. 2(b) we plot the characterization of  $S_q^{\text{GHZ}_2}(A|R)$  for the state  $\rho_{AR}^{\text{GHZ}_2}$ , given in Eq. (7), with the initial state chosen as the Bell state, with respect to  $\lambda$  for various values of  $q$ . We observe that, irrespective of the value of  $q$ , the nonseparability of  $\rho_{AR}^{\text{GHZ}_2}$  will be high at lower values of acceleration and decreases with the increase in acceleration; in particular,  $S_q^{\text{GHZ}_2}(A|R)$  tends to 0 as  $\lambda$  approaches 1. As the value of  $q$  increases, the AR  $q$ -conditional entropy suggests that the state  $\rho_{AR}^{\text{GHZ}_2}$  may transition towards separability in the limit  $\lambda \rightarrow 1$ . However,  $S_q^{\text{GHZ}_2}(A|R)$  approaching 0 becomes steeper at large values of both acceleration  $\lambda$  and the parameter  $q$ .

## 2. Generalized pure three-qubit GHZ state

Let us consider a generalized pure three-qubit GHZ state given by

$$|\text{GHZ}_3\rangle = \cos \theta |000\rangle + \sin \theta |111\rangle, \quad \cos^2 \theta + \sin^2 \theta = 1, \quad (14)$$

shared between Alice and Bob, with the first two of its qubits in Alice's possession while the remaining qubit is in Bob's possession, i.e., they belong to the  $H_{A_1} \otimes H_{A_2} \otimes H_B$  Hilbert space. By accelerating Bob's qubit, we study the nonseparability between inertial Alice's two qubits and Rob's modes in region I of Rindler space-time by exploring the AR  $q$ -conditional entropy. Using the recipe given in Sec. II, we get the composite state of the inertial  $A_1 A_2$  and noninertial  $R$  as  $\rho_{A_1 A_2 R_{\text{II}}}^{\text{GHZ}_3}$ , and the state  $\rho_{A_1 A_2 R}^{\text{GHZ}_3}$  as the mixed subsystem after tracing out the modes of Rob's qubit in region II. The density



matrix of  $\rho_{A_1 A_2 R}^{\text{GHZ}_3}$  is given by

$$\begin{aligned} \rho_{A_1 A_2 R}^{\text{GHZ}_3} = & \frac{1}{\cosh^2 r} \sum_{n=0}^{\infty} \tanh^{2n} r \left( \cos^2 \theta |00n\rangle \langle 00n| \right. \\ & + \frac{\sqrt{n+1}}{\cosh r} \cos \theta \sin \theta (|00n\rangle \langle 11n+1| \\ & + |11n+1\rangle \langle 00n|) \\ & \left. + \frac{n+1}{\cosh^2 r} \sin^2 \theta |11n+1\rangle \langle 11n+1| \right). \end{aligned} \quad (15)$$

Generally, there are two independent  $q$ -conditional entropies associated with arbitrary three-qubit states [58], which are given by

$$S_q(AB|C) = \frac{S_q^T(\rho_{ABC}) - S_q^T(\rho_C)}{1 + (1-q)S_q^T(\rho_C)} \quad (16)$$

and

$$S_q(A|BC) = \frac{S_q^T(\rho_{ABC}) - S_q^T(\rho_{BC})}{1 + (1-q)S_q^T(\rho_{BC})}, \quad (17)$$

where  $S_q^T(\rho_i)$  is the Tsallis  $q$  entropy of any state  $\rho_i$ . Since one of the qubits in the shared initial state is accelerating in a noninertial frame, a simultaneous measurement cannot be performed on the inertial and the noninertial qubits together. Hence, we choose the conditional entropy such that inertial Alice's qubits  $A_1$  and  $A_2$  are conditioned on noninertial Rob's modes  $R$ . Therefore, we proceed to investigate the separability using the AR  $q$ -conditional entropy  $S_q^{\text{GHZ}_3}(A_1 A_2 | R)$  in the  $A_1 A_2$ - $R$  bipartition for the state  $\rho_{A_1 A_2 R}^{\text{GHZ}_3}$  given in Eq. (15).

To get the eigenvalues of the states  $\rho_{A_1 A_2 R}^{\text{GHZ}_3}$  and  $\rho_R^{\text{GHZ}_3}$  to evaluate  $S_q^{\text{GHZ}_3}(A_1 A_2 | R)$ , we make use of the fact that their density matrices have the same nonzero eigenvalues as those of  $\rho_{AR}^{\text{GHZ}_2}$  and  $\rho_R^{\text{GHZ}_2}$ , respectively. Hence, the behavior of  $S_q^{\text{GHZ}_3}(A_1 A_2 | R)$  with respect to the state parameter  $\theta$ , acceleration  $\lambda$ , and  $q$  is exactly the same as the behavior of the AR  $q$ -conditional entropy for the pure two-qubit GHZ state with one of its qubit in acceleration  $S_q^{\text{GHZ}_2}(A | R)$  as given in Figs. 2(a) and 2(b). For logistical reasons, which will be clear later, we now study the nonseparability of the pure  $N$ -qubit GHZ state instead of the generalized  $N$ -qubit GHZ state.

### 3. Pure $N$ -qubit GHZ state

Here we generalize the characterization of the nonseparability of the pure GHZ states to the  $N$ -qubit GHZ state when one of its qubits is accelerated using the AR  $q$ -conditional entropy. Then the pure  $N$ -qubit GHZ state is given by

$$|\text{GHZ}_N\rangle = \frac{|0\rangle^{\otimes N} + |1\rangle^{\otimes N}}{\sqrt{2}}, \quad (18)$$

belonging to Hilbert space  $H_{A_1} \otimes H_{A_2} \otimes \cdots \otimes H_{A_{N-1}} \otimes H_B$ , i.e., the first  $N-1$  qubits are with Alice and the last qubit is in Bob's possession. The choice of the qubit, among pure  $N$ -qubit GHZ states, to be accelerated does not change the study of nonseparability among the inertial and noninertial qubits as the density-matrix structure of the composite state and its subsystem remain the same. When Bob accelerates,

the resulting composite state of inertial Alice and noninertial Rob, denoted by  $\rho_{A_1 A_2 \cdots A_{N-1} R_I R_{II}}^{\text{GHZ}_N}$ , is obtained by using the transformations from Minkowski to Rindler space-time given in Eqs. (1) and (2). Then  $\rho_{A_1 A_2 \cdots A_{N-1} R}^{\text{GHZ}_N}$ , after tracing out one of the disjoint regions in Rindler space-time (region II), is given by

$$\begin{aligned} \rho_{A_1 A_2 \cdots A_{N-1} R}^{\text{GHZ}_N} = & \frac{1}{2 \cosh^2 r} \sum_{n=0}^{\infty} \tanh^{2n} r \left( |00 \cdots 0n\rangle \langle 00 \cdots 0n| \right. \\ & + \frac{\sqrt{n+1}}{\cosh r} (|00 \cdots 0n\rangle \langle 11 \cdots 1n+1| \\ & + |11 \cdots 1n+1\rangle \langle 00 \cdots 0n|) \\ & \left. + \frac{n+1}{\cosh^2 r} |11 \cdots 1n+1\rangle \langle 11 \cdots 1n+1| \right). \end{aligned} \quad (19)$$

Rob's subsystem  $\rho_R^{\text{GHZ}_N}$  is equivalent to Eq. (11) with  $\theta = \pi/4$ . These two density matrices have the same nonzero eigenvalues as those of  $\rho_{AR}^{\text{GHZ}_2}$  and  $\rho_R^{\text{GHZ}_2}$  given in Eqs. (10) and (12) with  $\theta = \pi/4$ . Therefore, the behavior of the AR  $q$ -conditional entropy remains the same with respect to  $\lambda$  for various values of  $q$  as seen in Fig. 2(b). Increasing the number of qubits in the inertial frame does not affect the nonseparability behavior of the pure  $N$ -qubit GHZ state when any of its qubits is accelerated.

Hence, we can conclude that the pure multiqubit GHZ state with one of its qubits under acceleration always remains nonseparable throughout the range of  $\lambda$  and for any choice of  $q$ . The states are more nonseparable when the acceleration is low, and the nonseparability reduces as the acceleration increases, irrespective of the value of the parameter  $q$ . The nonseparability of the state in Eq. (19) approaching 0 becomes steeper for large values of  $\lambda$  and  $q$ .

## B. Pure multiqubit $W$ states

### 1. Generalized pure two-qubit $W$ state

A generalized pure two-qubit state  $|W_2\rangle$  shared between Alice and Bob in the inertial frame is given by

$$|W_2\rangle = \cos \theta |01\rangle + \sin \theta |10\rangle, \quad \cos^2 \theta + \sin^2 \theta = 1. \quad (20)$$

If we let Bob's qubit be relativistically accelerated with respect to Alice's qubit, the resulting composite state is  $\rho_{AR_I R_{II}}^{W_2}$ . Then the mixed density matrix  $\rho_{AR}^{W_2}$ , by following the recipe given in Sec. II, is given by

$$\begin{aligned} \rho_{AR}^{W_2} = & \frac{1}{\cosh^2 r} \sum_n \tanh^{2n} r \left( \frac{n+1}{\cosh^2 r} \cos^2 \theta |0n+1\rangle \langle 0n+1| \right. \\ & + \sin^2 \theta |1n\rangle \langle 1n| + \frac{\sqrt{n+1}}{\cosh r} \cos \theta \sin \theta (|0n+1\rangle \\ & \left. \times \langle 1n| + |1n\rangle \langle 0n+1|) \right). \end{aligned} \quad (21)$$

The structure of this state  $\rho_{AR}^{W_2}$  is made up of  $2 \times 2$  blocks along the diagonal, with the remaining off-diagonal elements being zero. This structure is the same as Eq. (8) but with the

nonzero blocks given by

$$\Delta_n(\rho_{AR}^{W_2}) = \tanh^{2n} r \begin{pmatrix} \alpha_n^2 \cos^2 \theta & \alpha_n \cos \theta \sin \theta \\ \alpha_n \cos \theta \sin \theta & \sin^2 \theta \end{pmatrix}. \quad (22)$$

Here  $\alpha_n = \frac{\sqrt{n+1}}{\cosh r}$ . The eigenvalues of this  $n$ th block of the state  $\rho_{AR}^{W_2}$  are 0 and

$$\Lambda'_n = \frac{\tanh^{2n} r}{\cosh^2 r} \left( \sin^2 \theta + \frac{n+1}{\cosh^2 r} \cos^2 \theta \right), \quad (23)$$

satisfying  $\text{Tr}(\rho_{AR}^{W_2}) = \sum_{n=0}^{\infty} \Lambda'_n = 1$ .

The marginal density matrix  $\rho_R^{W_2}$  is computed by tracing out the other subsystem  $A$  and is given by

$$\rho_R^{W_2} = \frac{1}{\cosh^2 r} \sum_{m=0}^{\infty} \tanh^{2m} r \left( \sin^2 \theta |m\rangle \langle m| + \frac{m+1}{\cosh^2 r} \cos^2 \theta |m+1\rangle \langle m+1| \right). \quad (24)$$

This is an infinite-dimensional diagonal matrix whose  $m$ th eigenvalue is given by

$$\Lambda'_m = \frac{\tanh^{2m} r}{\cosh^2 r} \left( \sin^2 \theta + \frac{m}{\sinh^2 r} \cos^2 \theta \right), \quad (25)$$

where  $\text{Tr}(\rho_R^{W_2}) = \sum_{m=0}^{\infty} \Lambda'_m = 1$ .

To characterize the nonseparability of the state of inertial Alice and noninertial Rob given in Eq. (21), we substitute the eigenvalues  $\Lambda'_n$  of  $\rho_{AR}^{W_2}$  and  $\Lambda'_m$  of  $\rho_R^{W_2}$  in the AR  $q$ -conditional entropy given in Eq. (5) to obtain

$$S_q^{W_2}(A|R) = \frac{1}{q-1} \left( 1 - \frac{\sum_{n=0}^{\infty} \left[ \tanh^{2n} r \left( \sin^2 \theta + \cos^2 \theta \frac{n+1}{\cosh^2 r} \right) \right]^q}{\sum_{m=0}^{\infty} \left[ \tanh^{2m} r \left( \sin^2 \theta + \cos^2 \theta \frac{m}{\sinh^2 r} \right) \right]^q} \right). \quad (26)$$

Using the eigenvalue truncation procedure introduced earlier, we choose a sufficiently large  $k \simeq 10^4$  and numerically compute the AR  $q$ -conditional entropy given in Eq. (26) and characterize the same with respect to the parameter  $q$ , the state parameter  $\theta$ , and Rob's acceleration  $\lambda$ . The  $S_q^{W_2}(A|R)$  always remains less than zero, implying that the state remains nonseparable for any values of  $\lambda$ ,  $\theta$ , and  $q$ . We observe that, irrespective of the value of  $q$ , the nonseparability of  $\rho_{AR}^{W_2}$  will be high at lower values of acceleration and decreases with the increase in acceleration. When  $\theta = \pi/4$ , Eq. (20) corresponds to a two-qubit Bell state in an inertial frame and the corresponding  $S_q^{W_2}(A|R)$  attains maximum nonseparability irrespective of the parameter  $q$ . These observations are similar to that of the two-qubit GHZ state given in Eq. (7), except the variation with respect to  $\cos^2 \theta$  in Fig. 2(a) is shifted in the case of  $\rho_{AR}^{W_2}$ . The characterization of  $S_q^{W_2}(A|R)$  for  $\rho_{AR}^{W_2}$  in Eq. (21) with the initial state being the Bell state, with respect to  $\lambda$  for various values of  $q$ , is the same as that given in Fig. 2(b).

## 2. Generalized pure three-qubit $W$ state

A generalized pure three-qubit  $W$  state, shared between Alice and Bob, is given by

$$|W_3\rangle = \sin \theta \cos \phi |001\rangle + \sin \theta \sin \phi |010\rangle + \cos \theta |100\rangle. \quad (27)$$

Let  $x = \sin \theta \cos \phi$ ,  $y = \sin \theta \sin \phi$ , and  $z = \cos \theta$ , giving  $x^2 + y^2 + z^2 = 1$ , which normalizes the given state for any  $\theta$  and  $\phi$ . Consider a scenario where the first two qubits belong to Alice, and Bob holds the third qubit. Subsequently, as Bob undergoes uniform acceleration (Rob) relative to Alice in an inertial frame, it gives rise to the composite state  $\rho_{A_1 A_2 R}^{W_3}$ . The final mixed state after tracing out Rob's mode in region II is expressed as

$$\rho_{A_1 A_2 R}^{W_3} = \frac{1}{\cosh^2 r} \sum_{n=0}^{\infty} \tanh^{2n} r \left[ \alpha_n^2 x^2 |00n+1\rangle \langle 00n+1| + xz\alpha_n (|00n+1\rangle \langle 10n| + |10n\rangle \langle 00n+1|) + xy\alpha_n (|00n+1\rangle \langle 01n| + |01n\rangle \langle 00n+1|) + z^2 |10n\rangle \langle 10n| + y^2 |01n\rangle \langle 01n| + yz(|10n\rangle \langle 01n| + |01n\rangle \langle 10n|) \right]. \quad (28)$$

The density matrix of this state  $\rho_{A_1 A_2 R}^{W_3}$  assumes a block structure along the diagonal as given in Eq. (8) and the remaining off-diagonal elements are zero. However, here the diagonal blocks are given by

$$\Delta_n(\rho_{A_1 A_2 R}^{W_3}) = \tanh^{2n} r \begin{pmatrix} y^2 & yz & 0 & xy\alpha_n \\ yz & z^2 & 0 & xz\alpha_n \\ 0 & 0 & 0 & 0 \\ xy\alpha_n & xz\alpha_n & 0 & x^2\alpha_n^2 \end{pmatrix}. \quad (29)$$

The nonzero eigenvalue of this  $n$ th block of the state  $\rho_{A_1 A_2 R}^{W_3}$  is given by

$$\delta_n = \frac{\tanh^{2n} r}{\cosh^2 r} \left( 1 + \frac{n+1 - \cosh^2 r}{\cosh^2 r} x^2 \right). \quad (30)$$

The reduced density matrix  $\rho_R^{W_3}$  corresponding to the modes of Rob in region I of the Rindler space-time is an infinite-dimensional diagonal matrix, with  $\delta_m$  as its diagonal elements. Then the  $m$ th eigenvalue of  $\rho_R^{W_3}$  is given by

$$\delta_m = \frac{\tanh^{2m} r}{\cosh^2 r} \left( 1 + \frac{m - \sinh^2 r}{\sinh^2 r} x^2 \right). \quad (31)$$

To characterize the nonseparability in the state  $\rho_{A_1 A_2 R}^{W_3}$  given in Eq. (28), we substitute these eigenvalues  $\delta_n$  and  $\delta_m$  in the expression for the AR  $q$ -conditional entropy for the  $A_1 A_2$ - $R$  bipartition to obtain

$$S_q^{W_3}(A_1 A_2 | R) = \frac{1}{q-1} \left( 1 - \frac{\sum_{n=0}^{\infty} \left[ \tanh^{2n} r \left( 1 + \frac{n+1 - \cosh^2 r}{\cosh^2 r} x^2 \right) \right]^q}{\sum_{m=0}^{\infty} \left[ \tanh^{2m} r \left( 1 + \frac{m - \sinh^2 r}{\sinh^2 r} x^2 \right) \right]^q} \right). \quad (32)$$

We are considering the nonseparability in the inertial-noninertial bipartition, as simultaneous measurements cannot

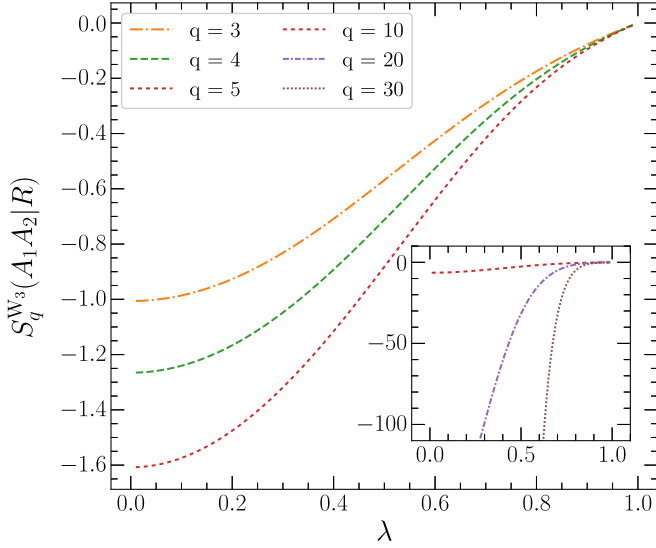


FIG. 3. Variation of the AR  $q$ -conditional entropy for the pure three-qubit  $W$  state as a function of the acceleration parameter  $\lambda$  for various values of  $q$ , with  $\theta = \cos^{-1}(1/\sqrt{3})$  and  $\phi = \pi/4$ .

be done in the other possible partitions. To compute this conditional entropy numerically, we use the eigenvalue truncation procedure and get  $k \simeq 10^4$ . Now, using these  $k$  eigenvalues of  $\rho_{A_1 A_2 R}^{W_3}$  and  $\rho_R^{W_3}$ , we numerically compute the AR  $q$ -conditional entropy in Eq. (32) and characterize the same with respect to its state parameters  $\theta$  and  $\phi$ , acceleration  $\lambda$ , and parameter  $q$ .

We observe that  $S_q^{W_3}(A_1 A_2 | R)$  consistently remains below zero, suggesting the nonseparability of the state for the entire range of system parameters, the acceleration  $\lambda$ , and the parameter  $q$ . The maximum nonseparability for the generalized pure three-qubit  $W$  state occurs for  $\theta$  and  $\phi$  such that  $\sin \theta \cos \phi = 1/\sqrt{2}$ . Moreover, to understand the behavior of  $S_q^{W_3}(A_1 A_2 | R)$  with respect to the other numerous parameters involved, we choose a pure three-qubit  $W$  state with equal coefficients, i.e., with state parameters  $\theta = \cos^{-1}(1/\sqrt{3})$  and  $\phi = \pi/4$ . Subsequently, the AR  $q$ -conditional entropy for this state is plotted as a function of the acceleration parameter  $\lambda$  in Fig. 3 for various values of  $q$ .

When Rob's acceleration is low, the nonseparability of the state  $\rho_{A_1 A_2 R}^{W_3}$  is most pronounced, as indicated by the minimum of  $S_q^{W_3}(A_1 A_2 | R)$ . However, with increasing acceleration, the conditional entropy increases and approaches 0 as  $\lambda$  tends to 1, for all values of  $q$ . As  $q$  increases,  $S_q^{W_3}(A_1 A_2 | R)$  becomes more negative for low  $\lambda$  but converges to 0 as  $\lambda$  tends to 1. Although the choices of  $\theta$  and  $\phi$  are not unique, the behavior of  $S_q^{W_3}(A_1 A_2 | R)$  with respect to  $\lambda$  will follow the same trend. However, these values of conditional entropy are higher than the corresponding conditional entropy for the generalized pure three-qubit GHZ state with one of its qubits in acceleration, hence indicating generalized pure three-qubit  $W$  states having weaker nonseparability than generalized pure three-qubit GHZ states with one of its qubits being accelerated. Similar to the case of pure multiqubit GHZ states, we only consider the pure  $N$ -qubit  $W$  state instead of the generalized pure  $N$ -qubit  $W$  state.

### 3. Pure $N$ -qubit $W$ state

A pure  $N$ -qubit  $W$  state, shared between Alice and Bob, is given by

$$|W_N\rangle = \frac{|00 \cdots 01\rangle + |00 \cdots 10\rangle + \cdots + |10 \cdots 00\rangle}{\sqrt{N}}, \quad (33)$$

where the first  $N - 1$  qubits are with Alice while the last qubit is in Bob's possession. Here we again consider only the pure  $N$ -qubit  $W$  state instead of the generalized  $N$ -qubit  $W$  state for logistical reasons. The final Alice-Rob state, after accelerating Bob's qubit and tracing out the second Rindler region of Rob's space-time using the recipe given in Sec. II, is given by

$$\begin{aligned} \rho_{A_1 A_2 \cdots A_{N-1} R}^{W_N} &= \frac{1}{N \cosh^2 r} \sum_{n=0}^{\infty} \tanh^{2n} r \{ \alpha_n^2 |00 \cdots 0n+1\rangle \langle 00 \cdots 0n+1| \\ &+ (|00 \cdots 1n\rangle + \cdots + |01 \cdots 0n\rangle + |10 \cdots 0n\rangle) \\ &\times (\langle 00 \cdots 1n| + \cdots + \langle 01 \cdots 0n| + \langle 10 \cdots 0n|) \\ &+ \alpha_n [ |00 \cdots 0n+1\rangle (\langle 00 \cdots 1n| + \cdots + \langle 01 \cdots 0n| \\ &+ \langle 10 \cdots 0n|) + \text{c.c.} ] \}. \end{aligned} \quad (34)$$

Since one of the qubits is accelerating in a noninertial frame, a simultaneous measurement cannot be done on the inertial and the noninertial qubits together. Hence we continue our investigation by choosing the  $A_1 A_2 \cdots A_{N-1} - R$  bipartition to calculate the AR  $q$ -conditional entropy  $S_q^{W_N}(A_1 A_2 \cdots A_{N-1} | R)$ . This conditional entropy is evaluated explicitly for the state given in Eq. (34), using the eigenvalues of the reduced system  $\rho_{A_1 A_2 \cdots A_{N-1} R}^{W_N}$  and its subsystem  $\rho_R^{W_N}$  and is given by

$$\begin{aligned} S_q^{W_N}(A_1 A_2 \cdots A_{N-1} | R) &= \frac{1}{q-1} \left( 1 - \frac{\sum_{n=0}^{\infty} \left[ \tanh^{2n} r \left( N-1 + \frac{n+1}{\cosh^2 r} \right) \right]^q}{\sum_{m=0}^{\infty} \left[ \tanh^{2m} r \left( N-1 + \frac{m}{\sinh^2 r} \right) \right]^q} \right). \end{aligned} \quad (35)$$

This conditional entropy  $S_q^{W_N}(A_1 A_2 \cdots A_{N-1} | R)$  can be numerically computed for various values of  $N$ ,  $\lambda$ , and  $q$  using the eigenvalue truncation procedure given previously. With  $k \simeq 10^4$ , the  $S_q^{W_N}(A_1 A_2 \cdots A_{N-1} | R)$  is found to be again nonseparable throughout the ranges of the system parameters, acceleration  $\lambda$ , and  $q$ . The conditional entropy is plotted for various values of  $N$  and  $\lambda$  for  $q = 2$  in Fig. 4. We observe that irrespective of  $N$ , the nonseparability of  $\rho_{A_1 A_2 \cdots A_{N-1} R}^{W_N}$  is high at lower values of acceleration and decreases with the increase in acceleration as  $S_q^{W_N}(A_1 A_2 \cdots A_{N-1} | R)$  tends to 0 when  $\lambda$  reaches 1. However, as  $N$  increases, the variation of  $S_q^{W_N}(A_1 A_2 \cdots A_{N-1} | R)$  with respect to  $\lambda$  becomes less steep. Hence, we can conclude that the nonseparability of the state  $\rho_{A_1 A_2 \cdots A_{N-1} R}^{W_N}$  is reduced as the number of qubits in the inertial subsystem increases. This observation remains true for all values of the parameter  $q$ .

To summarize, all the pure multiqubit GHZ and  $W$  states with one of its qubits under acceleration will remain nonseparable in the inertial-noninertial bipartition throughout the ranges of its state parameters, the parameter  $q$ , and acceleration  $\lambda$ . The states are highly nonseparable at low acceleration

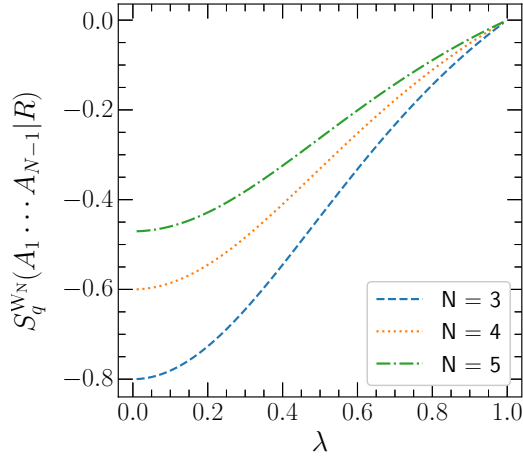


FIG. 4. Variation of the AR  $q$ -conditional entropy of the pure  $N$ -qubit  $W$  state as a function of the acceleration  $\lambda$  for different values of  $N$ , with  $q = 2$ .

$\lambda$  and tend towards separability at very high acceleration of  $\lambda$  tending to 1. Moreover, with one of its qubits under acceleration, the nonseparability of the pure multiqubit GHZ and  $W$  states becomes steeper while approaching 0 at large values of acceleration  $\lambda$  and the parameter  $q$ . The nonseparability of the pure  $N$ -qubit GHZ state with one of its qubits being accelerated is independent of the number of qubits  $N$ , while for the pure  $N$ -qubit  $W$  state, the nonseparability decreases with an increase in the number of qubits. Consequently, the pure  $N$ -qubit  $W$  state with one of its qubits under acceleration has weaker nonseparability than the pure  $N$ -qubit GHZ state with one of its qubits under acceleration.

## V. MIXED MULTIQUBIT STATES WITH AN ACCELERATING QUBIT

In this section we introduce a global noise to all the pure states considered in Sec. IV when they have equal probability in their superposed states and study the nonseparability of resultant mixed states when one of its qubits is accelerated, using the AR  $q$ -conditional entropy. The nonseparability of the mixed states with an accelerating qubit thus obtained is characterized with respect to the parameter  $q$ , acceleration parameter  $\lambda$ , and mixing parameter  $p$ .

### A. Mixed multiqubit GHZ states

#### 1. Mixed two-qubit GHZ state

A mixed two-qubit GHZ state shared between Alice and Bob, obtained by adding a global noise to the pure two-qubit GHZ state, is given by

$$\varrho_{AB}^{\text{GHZ}_2} = \frac{p}{4} \mathbb{I}_d + (1-p) |\psi_{AB}\rangle \langle \psi_{AB}|, \quad (36)$$

where  $|\psi_{AB}\rangle = (|00\rangle + |11\rangle)/\sqrt{2}$ ,  $\mathbb{I}_d$  is the  $4 \times 4$  identity matrix, and  $p$  is the global noise or the mixing parameter. Note that  $p$  is a parameter in the range  $[0, 1]$ ;  $p = 0$  denotes the pure two-qubit GHZ state and  $p = 1$  denotes the maximally mixed two-qubit GHZ state. Let us consider that Bob is now relativistically accelerating with respect to Alice and the

resulting composite state is  $\varrho_{AR_I R_{II}}^{\text{GHZ}_2}$ . We now obtain the reduced state of Alice and Rob in region I by tracing out Rob's mode in region II, using the recipe given in Sec. II, as

$$\begin{aligned} \varrho_{AR}^{\text{GHZ}_2} &= \frac{1}{\cosh^2 r} \sum_{n=0}^{\infty} \tanh^{2n} r \\ &\times \left[ \frac{2-p}{4} \left( |0n\rangle \langle 0n| + \frac{n+1}{\cosh^2 r} |1n+1\rangle \langle 1n+1| \right) \right. \\ &+ \frac{p}{4} \left( |1n\rangle \langle 1n| + \frac{n+1}{\cosh^2 r} |0n+1\rangle \langle 0n+1| \right) \\ &\left. + \frac{1-p}{2} \frac{\sqrt{n+1}}{\cosh r} (|0n\rangle \langle 1n+1| + |1n+1\rangle \langle 0n|) \right]. \end{aligned} \quad (37)$$

Rob's subsystem in region I, by tracing out Alice's qubit, is given by

$$\begin{aligned} \varrho_R^{\text{GHZ}_2} &= \frac{1}{2 \cosh^2 r} \sum_{n=0}^{\infty} \tanh^{2n} r \\ &\times \left( |n\rangle \langle n| + \frac{n+1}{\cosh^2 r} |n+1\rangle \langle n+1| \right). \end{aligned} \quad (38)$$

These infinite-dimensional density matrices do not possess a block-diagonal structure; hence, arriving at the analytical form for their eigenvalues is not straightforward and one has to resort to numerical techniques. Below, we describe a procedure for obtaining the eigenvalues of these two density matrices to evaluate the AR  $q$ -conditional entropy.

*Density-matrix truncation procedure.* To numerically compute the AR  $q$ -conditional entropy, we make use of the fact that the sum of the eigenvalues of  $\varrho_{AR}^{\text{GHZ}_2}$  and  $\varrho_R^{\text{GHZ}_2}$  tends to 1 as  $n$  and  $m$  approach infinity, respectively. However, unlike the case of pure states, we do not have the analytical expression for  $\mathcal{S}_q^{W_2}(A|R)$  in terms of the eigenvalues of  $\varrho_{AR}^{\text{GHZ}_2}$  and  $\varrho_R^{\text{GHZ}_2}$ . Therefore, we use the numerical technique in which the matrix dimension of infinity is approximated to an agreeable finite dimension  $l \times l$  of the density matrix such that  $\text{Tr}(\varrho_{AR}^{\text{GHZ}_2})$  approaches 1. For the density matrix given in Eq. (37), the dimension of  $\varrho_{AR}^{\text{GHZ}_2}$  for which  $\text{Tr}(\varrho_{AR}^{\text{GHZ}_2})$  approaches 1 is found to be around  $l \approx 10^3$ . Similarly, eigenvalues are also obtained for Rob's subsystem in region I,  $\varrho_R^{\text{GHZ}_2}$ , by limiting its dimension to finite  $l \times l$  such that  $\text{Tr}(\varrho_R^{\text{GHZ}_2})$  approaches 1.

Now the AR  $q$ -conditional entropy is numerically computed for the state given in Eq. (37) using the density-matrix truncation procedure described above, for various values of Rob's acceleration  $\lambda$ , the mixing parameter  $p$ , and the parameter  $q$ . The AR  $q$ -conditional entropy for the initial mixed state whose subsystem is accelerated is given by  $\mathcal{S}_q^{\text{GHZ}_2}(A|R)$ . It is plotted as a function of the acceleration  $\lambda$  and parameter  $p$  in Fig. 5(a) for  $q = 2$ . We can observe that in the plot of  $\mathcal{S}_q^{\text{GHZ}_2}(A|R)$  for the state given in Eq. (37), there exist regions of both separability (red shades) and nonseparability (blue shades) depending on the choices of  $\lambda$  and  $p$ . The  $\mathcal{S}_q^{\text{GHZ}_2}(A|R) = 0$  (black dotted) curve indicates the transition of  $\varrho_{AR}^{\text{GHZ}_2}$  from nonseparability to separability and it depends on values of  $\lambda$  and  $p$ . The whole transition curve shifts towards the right as  $q$  increases, indicating that with an increase in the



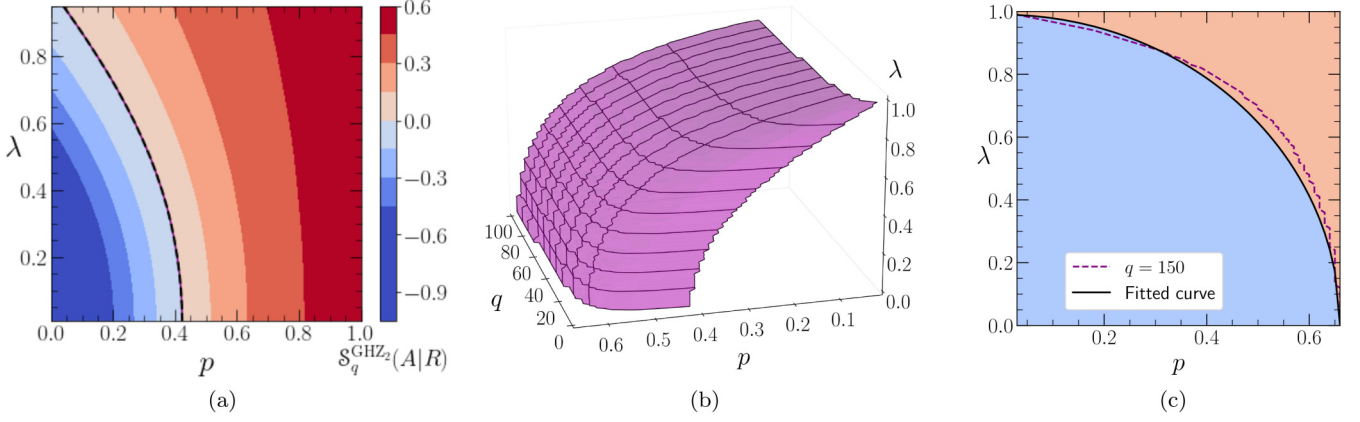


FIG. 5. (a) Variation of the Abe-Rajagopal  $q$ -conditional entropy of a single-qubit-accelerated mixed two-qubit GHZ state as a function of  $p$  and  $\lambda$  for  $q = 2$ . The black solid line corresponds to the transition from negative to positive AR  $q$ -conditional entropy. (b) Variation of the mixing parameter  $p$  for which  $\mathcal{S}_q^{\text{GHZ}_2}(A|R) = 0$ , with respect to  $q$  for the acceleration parameter  $\lambda$ . We can observe that the values of the mixing parameter saturate as  $q \rightarrow \infty$  for a given acceleration  $\lambda$ . (c) Variation of the mixing parameter  $p$  for which  $\mathcal{S}_q^{\text{GHZ}_2}(A|R) = 0$ , with respect to the acceleration parameter  $\lambda$  for  $q = 150$ . The blue region denotes the region where the state remains nonseparable, while the red region denotes the separability.

$q$  value, the area of the nonseparability region with respect to  $\lambda$  and  $p$  keeps increasing. As  $q$  is increased to large values, say, 50 and above, the transition curve becomes saturated with respect to  $\lambda$  and  $p$  as interpreted from Fig. 5(b). Hence, the strongest condition for separability can be obtained in the asymptotic limit of  $q$  tending to  $\infty$  ( $q \rightarrow \infty$ ).

For the asymptotic limit of  $q \rightarrow \infty$ , in Fig. 5(c) we plot the transition point from nonseparability to separability obtained numerically, i.e.,  $\mathcal{S}_q^{\text{GHZ}_2}(A|R) = 0$  with respect to  $p$  and  $\lambda$  (dashed curve). Note that the saturation occurs beyond  $q = 50$ , and we choose a reasonably high value of  $q = 150$  to study separability. The blue-shaded region denotes the nonseparable states, while the red-shaded region denotes the separable states. These transition points for different acceleration can be fitted to a curve of the form

$$(p/b)^x + \lambda^y = 1. \quad (39)$$

The choice of the function for the fitted curve is made using the fact that the separability occurs at  $p = b$  when the acceleration  $\lambda = 0$  and at  $p = 0$  as the acceleration  $\lambda \rightarrow 1$ . Hence, the separability criterion for the state in Eq. (37), which relates the mixing parameter  $p$  and Rob's acceleration  $\lambda$ , is given by

$$p > \frac{2}{3}(1 - \lambda^{2.2})^{(1/2.05)}. \quad (40)$$

When Rob's acceleration  $\lambda = 0$ , the necessary and sufficient condition for separability of this state occurs at  $p > \frac{2}{3}$  [70],

which is recovered from Eq. (40). As the acceleration increases, the nonseparable region keeps decreasing, and the nonseparability vanishes only at acceleration  $\lambda$  approaching 1. Hence, Eq. (40) gives the strongest condition for separability in the asymptotic limit of  $q$  for the mixed two-qubit GHZ state with one of its qubits being accelerated.

## 2. Mixed $N$ -qubit GHZ state

We add a global noise to the pure  $N$ -qubit GHZ state to obtain a mixed  $N$ -qubit GHZ state, which is shared between two parties Alice and Bob in the inertial frame, where Alice has the first  $N - 1$  qubits and Bob has the  $N$ th qubit in his possession. This state is given by

$$\rho_{A_1 A_2 \dots A_{N-1} B}^{\text{GHZ}_N} = \frac{p}{2^N} \mathbb{I}_d + (1-p) |\psi_{A_1 A_2 \dots A_{N-1} B}\rangle \langle \psi_{A_1 A_2 \dots A_{N-1} B}|, \quad (41)$$

where  $|\psi_{A_1 A_2 \dots A_{N-1} B}\rangle = (|0\rangle^{\otimes N} + |1\rangle^{\otimes N})/\sqrt{2}$ ,  $\mathbb{I}_d$  is the  $2^N \times 2^N$  identity matrix, and  $p$  is the mixing parameter. Let us now consider that Bob is uniformly accelerating with respect to Alice and the resulting state  $\rho_{A_1 A_2 \dots A_{N-1} R_I}^{\text{GHZ}_N}$  is obtained by using the transformations from Minkowski to Rindler space-time in Eqs. (1) and (2). The final state  $\rho_{A_1 A_2 \dots A_{N-1} R}^{\text{GHZ}_N}$  shared between Alice and Rob's mode in the region I is obtained using the recipe given in Sec. II and is given by

$$\begin{aligned} \rho_{A_1 A_2 \dots A_{N-1} R}^{\text{GHZ}_N} = & \frac{1}{\cosh^2 r} \sum_{n=0}^{\infty} \tanh^{2n} r \left( \frac{2-p}{2^N} [(|00 \dots n\rangle + |01 \dots n\rangle + \dots + |11 \dots n\rangle) \langle 00 \dots n| + \langle 01 \dots n| + \dots + \langle 11 \dots n|] \right. \\ & + \alpha_n^2 (|00 \dots n+1\rangle + |01 \dots n+1\rangle + \dots + |11 \dots n+1\rangle) \langle 00 \dots n+1| + \langle 01 \dots n+1| \\ & + \dots + \langle 11 \dots n+1|] + \frac{1-p}{2} [ |00 \dots 0n\rangle \langle 00 \dots 0n| + \alpha_n (|00 \dots 0n\rangle \langle 11 \dots 1n+1| \\ & \left. + |11 \dots 1n+1\rangle \langle 00 \dots 0n|) + \alpha_n^2 |11 \dots 1n+1\rangle \langle 11 \dots 1n+1| \right]. \end{aligned} \quad (42)$$

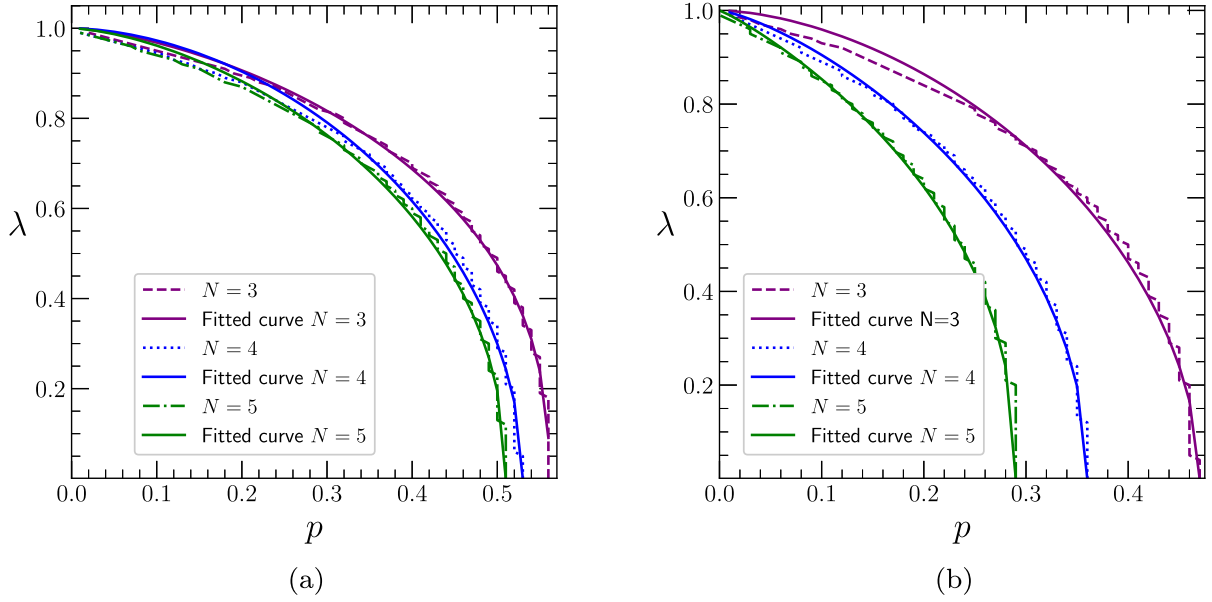


FIG. 6. Variation of the nonseparable to separable transition points of the AR  $q$ -conditional entropy for the (a) mixed  $N$ -qubit GHZ state and (b) mixed  $N$ -qubit  $W$  state, with one of its qubits in uniform acceleration, as a function of the acceleration parameter  $\lambda$  and mixing parameter  $p$  for  $N = 3, 4$ , and  $5$ . The fitted curves are shown by the colored solid lines.

Rob's subsystem is obtained by tracing out inertial Alice's qubits, i.e.,

$$\rho_R^{\text{GHZ}_N} = \text{Tr}_{A_1 A_2 \dots A_{N-1}} (\rho_{A_1 A_2 \dots A_{N-1} R}^{\text{GHZ}_N}).$$

Using the density-matrix truncation procedure given in the preceding section, we can numerically obtain the AR  $q$ -conditional entropy  $\mathcal{S}_q^{\text{GHZ}_N}(A_1 A_2 \dots A_{N-1} | R)$  in the inertial-noninertial bipartition for any choice of  $N$ . For example, when a mixed three-qubit GHZ state with one of its qubits under acceleration is considered (see Sec. 1 in the Appendix), we observe a transition from nonseparability to separability depending on the values of acceleration  $\lambda$ , the parameter  $q$ , and the mixing parameter  $p$ . In the asymptotic limit of  $q \rightarrow \infty$ , the transition from nonseparability to separability saturates to a curve, which is fitted to the function given in Eq. (39). Then the separability criterion for the state  $\rho_{A_1 A_2 R}^{\text{GHZ}_3}$  [see Eq. (A2)], in terms of the mixing parameter, is given as

$$p > 0.56(1 - \lambda^{2.47})^{(1/1.49)}. \quad (43)$$

Here the separability occurs at  $p = 0.56$  when the acceleration  $\lambda = 0$  and it reduces to  $p = 0$  when  $\lambda = 1$ , indicating that the region of nonseparability decreases with an increase in acceleration for the three-qubit mixed GHZ state with one of its qubits being accelerated.

A similar investigation is performed for mixed multiqubit GHZ states with  $N = 4$  and  $5$  when one of their qubits is accelerated. The nonseparability to separability transition with respect to  $\lambda$  and  $p$  in the asymptotic limit of  $q \rightarrow \infty$  is observed to be similar to the  $N = 3$  case. To study the impact of  $N$  on the nonseparability to separability transition, we plot  $\mathcal{S}_q^{\text{GHZ}_N}(A_1 A_2 \dots A_{N-1} | R) = 0$  with respect to  $p$  and  $\lambda$  for  $N = 3, 4$ , and  $5$  in Fig. 6(a). The strongest condition for separability obtained in the asymptotic limit of  $q \rightarrow \infty$  for these states is fitted to the family of curves in Eq. (39). The nonseparability region of mixed  $N$ -qubit GHZ states with

one of its qubits under acceleration decreases as  $N$  increases. The states tend to become separable for all choices of  $N$  as the acceleration  $\lambda$  approaches 1. These separability conditions for the different mixed  $N$ -qubit GHZ states with one of their qubits being accelerated ( $N = 2, 3, 4$ , and  $5$ ) are consolidated in Table I.

## B. Mixed multiqubit $W$ states

### 1. Mixed two-qubit $W$ state

A mixed two-qubit state shared between Alice and Bob, obtained by introducing a global noise to the pure two-qubit  $W$  state, is given by

$$\rho_{AB}^{W_2} = \frac{p}{4} \mathbb{I}_d + (1-p) |\psi_{AB}\rangle \langle \psi_{AB}|, \quad (44)$$

where  $|\psi_{AB}\rangle = (|01\rangle + |10\rangle)/\sqrt{2}$ ,  $\mathbb{I}_d$  is the  $4 \times 4$  identity matrix, and  $p$  is the mixing parameter. Let us consider that Bob is now relativistically accelerating with respect to Alice and the resulting composite state is  $\rho_{AR_1 R_{II}}^{W_2}$ . We now obtain the reduced state of Alice and Rob in region I by tracing out Rob's mode in region II, using a recipe given in Sec. II, as

$$\begin{aligned} \rho_{AR}^{W_2} &= \frac{1}{\cosh^2 r} \sum_{n=0}^{\infty} \tanh^{2n} r \\ &\times \left[ \frac{2-p}{4} \left( |1n\rangle \langle 1n| + \frac{n+1}{\cosh^2 r} |0n+1\rangle \langle 0n+1| \right) \right. \\ &+ \frac{p}{4} \left( |0n\rangle \langle 0n| + \frac{n+1}{\cosh^2 r} |1n+1\rangle \langle 1n+1| \right) \\ &\left. + \frac{1-p}{2} \frac{\sqrt{n+1}}{\cosh r} (|0n+1\rangle \langle 1n| + |1n\rangle \langle 0n+1|) \right]. \end{aligned} \quad (45)$$

TABLE I. Conditions for separability obtained using the AR  $q$ -conditional entropy for multiqubit GHZ and  $W$  states. The pure multiqubit states with one of its qubits in acceleration remain nonseparable (NS) everywhere. The conditions for mixed GHZ and  $W$  states fit the family of curves given in Eq. (39).

$N$	Pure $\rho_{AR}^{\text{GHZ}_N} / \rho_{AR}^{W_N}$	Mixed $\rho_{AR}^{\text{GHZ}_N}$	Mixed $\rho_{AR}^{W_N}$
2	NS	$\frac{2}{3}(1 - \lambda^{2.2})^{(1/2.05)}$	$\frac{2}{3}(1 - \lambda^{1.57})^{(1/2.6)}$
3	NS	$p > 0.56(1 - \lambda^{2.47})^{(1/1.49)}$	$p > 0.47(1 - \lambda^{1.86})^{(1/1.68)}$
4	NS	$p > 0.53(1 - \lambda^{1.92})^{(1/1.78)}$	$p > 0.36(1 - \lambda^{2.04})^{(1/1.32)}$
5	NS	$p > 0.51(1 - \lambda^{2.14})^{(1/1.55)}$	$p > 0.29(1 - \lambda^{2.28})^{(1/1.12)}$

Rob's subsystem  $\rho_R^{W_2}$  is obtained by tracing out inertial Alice's qubits from the state  $\rho_{AR}^{W_2}$  and is the same as  $\rho_R^{\text{GHZ}_2}$  given in Eq. (38). Now, using the density-matrix truncation procedure given in Sec. V A, the conditional entropy  $\mathcal{S}_q^{W_2}(A|R)$  can be numerically evaluated for this state. The characterization of  $\mathcal{S}_q^{W_2}(A|R)$  for this state qualitatively remains the same as given in Figs. 5(a) and 5(b) for the mixed two-qubit GHZ state with one of its qubit in acceleration, but differ in values. The nonseparability to separability transition for this state in the asymptotic limit of  $q$  can also be fitted to the function given in Eq. (39). Thus, the separability criterion in terms of the mixing parameter and acceleration  $\lambda$  for  $\rho_{AR}^{W_2}$  is given by

$$p > \frac{2}{3}(1 - \lambda^{1.57})^{(1/2.6)}, \quad (46)$$

indicating that when  $\lambda = 0$  we get  $p > \frac{2}{3}$  as the separable region and the separable region increases as  $\lambda$  increases. The mixing parameter  $p$  above which the state is separable tends to 0 as the acceleration  $\lambda$  tends to 1 in the asymptotic limit of  $q$ .

$$\begin{aligned} \rho_{A_1 A_2 \dots A_{N-1} R}^{W_N} &= \frac{1}{\cosh^2 r} \sum_{n=0}^{\infty} \tanh^{2n} r \left( \frac{2-p}{2^N} [(|00 \dots n\rangle + |01 \dots n\rangle + \dots + |11 \dots n\rangle)(\langle 00 \dots n| + \langle 01 \dots n| + \dots + \langle 11 \dots n|) \right. \\ &+ \alpha_n^2 (|00 \dots n+1\rangle + |01 \dots n+1\rangle + \dots + |11 \dots n+1\rangle)(\langle 00 \dots n+1| + \langle 01 \dots n+1| \\ &+ \dots + \langle 11 \dots n+1|)] + \frac{1-p}{N} \{ \alpha_n^2 |00 \dots 0n+1\rangle \langle 00 \dots 0n+1| + \alpha_n [ |00 \dots 0n+1\rangle \langle 00 \dots 1n| \\ &+ \dots + \langle 10 \dots 0n|] + (|00 \dots 1n\rangle + \dots + |10 \dots 0n\rangle) \langle 00 \dots 0n+1| \\ &+ (|00 \dots 1n\rangle + \dots + |10 \dots 0n\rangle)(\langle 00 \dots 1n| + \dots + \langle 10 \dots 0n|) \} \Big). \end{aligned} \quad (48)$$

Rob's subsystem  $\rho_R^{W_N}$  is obtained by tracing out inertial Alice's qubits. We can numerically obtain the AR  $q$ -conditional entropy  $\mathcal{S}_q^{W_N}(A_1 A_2 \dots A_{N-1} | R)$  in the inertial-noninertial bipartition, using the density-matrix truncation procedure given in Sec. V A for any choice of  $N$ . For example, when  $N = 3$ , a mixed three-qubit  $W$  state with one of its qubits under acceleration, is considered (see Sec. 2 in the Appendix), depending on the values of acceleration  $\lambda$ , the parameter  $q$ , and the mixing parameter  $p$ , we observe a transition from nonseparability to separability. This transition saturates to a curve in the asymptotic limit  $q \rightarrow \infty$ , which is fitted to the function given in Eq. (39). Then the separability criterion for the state  $\rho_{A_1 A_2 R}^{W_3}$  given in Eq. (A4), in terms of the mixing parameter  $p$

## 2. Mixed $N$ -qubit $W$ state

We get a mixed  $N$ -qubit  $W$  state by introducing a global noise to the pure  $N$ -qubit  $W$  state, which is given by

$$\rho_{A_1 A_2 \dots A_{N-1} B}^{W_N} = \frac{p}{2^N} \mathbb{I}_d + (1-p) |\psi_{A_1 A_2 \dots A_{N-1} B}\rangle \langle \psi_{A_1 A_2 \dots A_{N-1} B}|, \quad (49)$$

where  $|\psi_{A_1 A_2 \dots A_{N-1} B}\rangle = (|00 \dots 01\rangle + |00 \dots 10\rangle + \dots + |10 \dots 00\rangle) / \sqrt{N}$ ,  $\mathbb{I}_d$  is the  $2^N \times 2^N$  identity matrix, and  $p$  is the mixing parameter. In the inertial frame, this state is shared between the two parties Alice and Bob, where Alice has the first  $N-1$  qubits and Bob has  $N$ th qubit in his possession. Let us now consider that Bob is now uniformly accelerated with respect to Alice and the resulting state  $\rho_{A_1 A_2 \dots A_{N-1} R_{\text{II}}}^{W_N}$  is obtained by using the transformations from Minkowski to Rindler space-time given in Eqs. (1) and (2). The final state  $\rho_{A_1 A_2 \dots A_{N-1} R}^{W_N}$  between Alice and Rob's modes in region I using the recipe given in Sec. II is given by

and  $\lambda$ , is

$$p > 0.47(1 - \lambda^{1.86})^{(1/1.68)}, \quad (49)$$

implying that  $p > 0.47$  is a separable region when  $\lambda = 0$ ; as  $\lambda$  tends to 1, the state remains separable irrespective of the value of mixing parameter  $p$ .

Further, we observe a similar nonseparability to separability transition with respect to  $\lambda$  and  $p$  in the asymptotic limit of  $q \rightarrow \infty$  for  $N = 4$  and 5. In Fig. 6(b) we plot  $\mathcal{S}_q^{\text{GHZ}_N}(A_1 A_2 \dots A_{N-1} | R) = 0$  with respect to  $p$  and  $\lambda$  for  $N = 3, 4$ , and 5. These separability to nonseparability transitions are fitted to the family of curves in Eq. (39). We can observe that the nonseparability region is reduced as  $N$

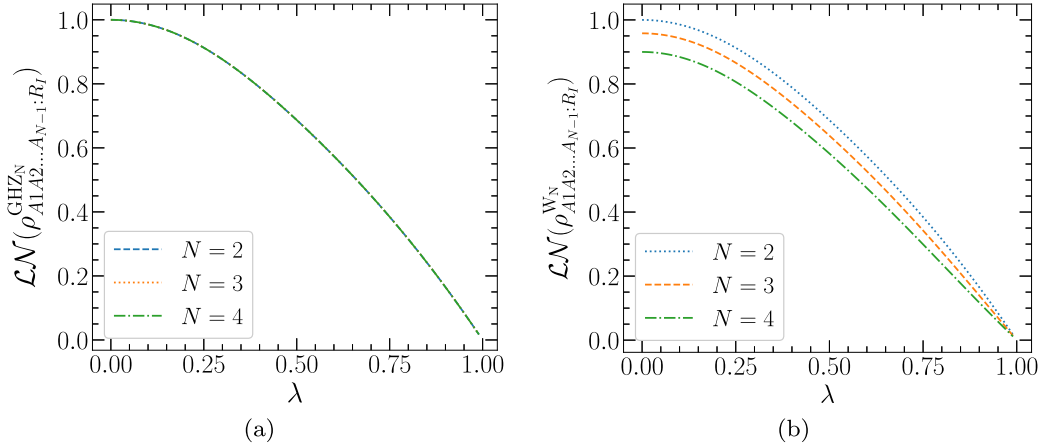


FIG. 7. Variation of the logarithmic negativity of the single-qubit-accelerated pure  $N$ -qubit (a) GHZ state and (b)  $W$  state as a function of the acceleration  $\lambda$  for different numbers of qubits  $N$  in these states.

increases. Moreover, this reduction is much faster than its mixed  $N$ -qubit GHZ counterpart, indicating that mixed  $N$ -qubit GHZ states can sustain nonseparability better than mixed  $N$ -qubit  $W$  states when one of their qubits is uniformly accelerated with respect to others. The consolidated conditions for separability of single-qubit-accelerated mixed multiqubit GHZ and  $W$  states are presented in Table I.

## VI. AR $q$ -CONDITIONAL ENTROPY AND LOGARITHMIC NEGATIVITY

We now draw a comparison between the nonseparability obtained through AR  $q$ -conditional entropy and the entanglement measure, viz., logarithmic negativity [71,72]. Logarithmic negativity for the state  $\rho_{AR_I}$  in the inertial-noninertial bipartition can be defined as

$$\mathcal{LN}(\rho_{A:R_I}) = \log_2 \|\rho_{AR_I}^{T_{R_I}}\|_1, \quad (50)$$

where  $T_{R_I}$  is the partial transpose taken over the subsystem  $\rho_{R_I}$  and  $\|\cdot\|$  gives the trace norm. In addition,  $\mathcal{LN}(\rho_{AB}) = 0$  for separable states and  $\mathcal{LN}(\rho_{AB}) > 0$  for entangled states. Further, the definition of logarithmic negativity can be extended to the single-qubit-accelerated  $N$ -qubit state as

$$\mathcal{LN}(\rho_{A_1 A_2 \dots A_{N-1} : R_I}) = \log_2 \|\rho_{A_1 A_2 \dots A_{N-1} R_I}^{T_{R_I}}\|_1, \quad (51)$$

where the bipartition is considered between inertial Alice's particles  $A_1, A_2, \dots, A_{N-1}$  and noninertial Rob's mode  $R_I$ .

It has been shown that the logarithmic negativity for a single-qubit-accelerated maximally entangled two-qubit state degrades as acceleration increases and it tends to zero in the infinite-acceleration limit [9]. Here we characterize the behavior of logarithmic negativity [see Eq. (51)] in single-qubit-accelerated  $N$ -qubit pure GHZ and  $W$  states given in Eqs. (19) and (34), respectively. The variation of logarithmic negativity for single-qubit-accelerated  $N$ -qubit pure GHZ

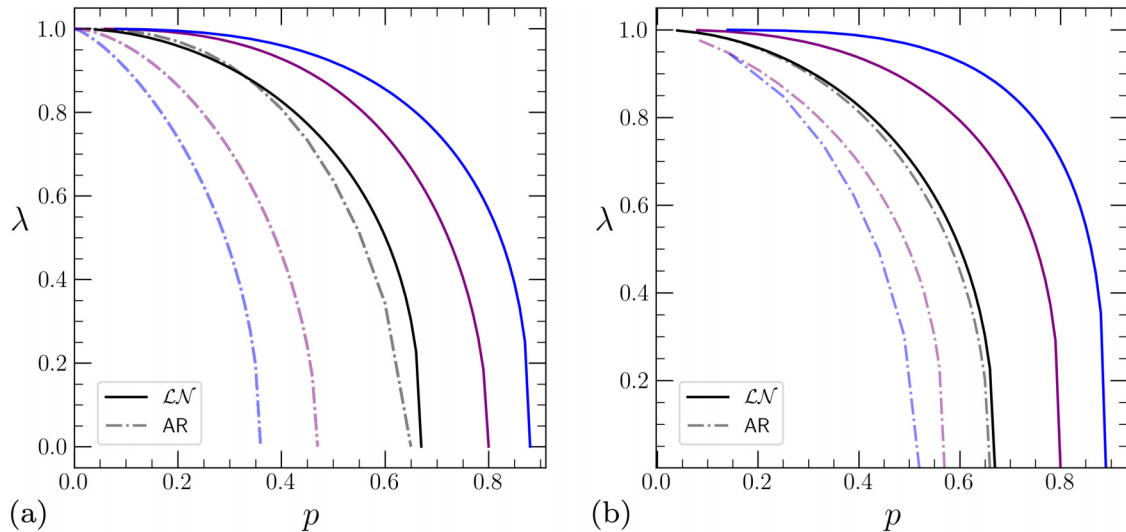


FIG. 8. Transitions from nonseparability to separability using AR  $q$ -conditional entropy (dash-dotted curves) and entanglement to separability using the logarithmic negativity (solid curves) for the single-qubit-accelerated  $N$ -qubit mixed (a) GHZ state and (b)  $W$  state as a function of the acceleration parameter  $\lambda$  and mixing parameter  $p$ . Here the numbers of qubits in the system are  $N = 2$  (black), 3 (violet), and 4 (blue).



and  $W$  states (for  $N = 2, 3$ , and  $4$ ) with respect to the acceleration  $\lambda$  is plotted in Figs. 7(a) and 7(b), respectively. The entanglement for a single-qubit-accelerated  $N$ -qubit pure GHZ state is independent of the number of qubits in the system, whereas entanglement decreases as the number of qubits increases for a single-qubit-accelerated  $N$ -qubit pure  $W$  state. However, the entanglement in both these pure multi-qubit states reduces as acceleration  $\lambda$  increases and goes to zero at infinite acceleration. The AR  $q$ -conditional entropy of single-particle-accelerated  $N$ -qubit pure GHZ and  $W$  states also shows the same behavior for nonseparability such that the nonseparability reduces as acceleration increases and the state tends towards separability in the infinite-acceleration limit.

The logarithmic negativity for a single-qubit-accelerated two-, three-, and  $N$ -qubit mixed GHZ state [given in Eqs. (37), (A2), and (42)] and  $W$  state [given in Eqs. (45), (A4), and (48)] in the inertial-noninertial bipartition can be evaluated using its definition given in Eq. (51). The entanglement to separability transition in these states as a function of the acceleration and mixing parameter  $p$  is given in Figs. 8(a) and 8(b). For any  $N$ , all multiqubit mixed states for which the logarithmic negativity lies under the transition curve represent the entangled states, whereas those with logarithmic negativity above the transition curve represent the separable states. For  $N = 2$ , the transition curves obtained from AR  $q$ -conditional entropy and logarithmic negativity are equivalent for both mixed GHZ and  $W$  states. However, as  $N$  increases, the entanglement to separability transition from logarithmic negativity is obtained at higher mixing parameter  $p$  for a particular acceleration  $\lambda$ , whereas the nonseparability to separability transition from AR  $q$ -conditional entropy occurs at a lower  $p$  for the same  $\lambda$  [see Figs. 6(a) and 6(b)]. Strikingly, the entanglement (nonseparability) provided by the logarithmic negativity (AR  $q$ -conditional entropy) for the single-qubit-accelerated  $N$ -qubit mixed GHZ state is stronger than that of the single-qubit-accelerated  $N$ -qubit mixed  $W$  state. Therefore, we can conclude that the AR  $q$ -conditional entropy of single-particle-accelerated mixed multiqubit GHZ and  $W$  states provides a more robust condition for nonseparability than the logarithmic negativity as the number of qubits in the system increases.

### VII. CONCLUSION

In an inertial frame, a shared state between two parties Alice and Bob,  $\rho_{AB}$ , can be represented using Minkowski coordinates. When Bob undergoes a uniform acceleration, the vacuum and excited states in Minkowski coordinates transform into the corresponding two-mode squeezed-vacuum states in Rindler coordinates. The two modes of this accelerated Bob (Rob) state belong to the two disjoint regions of the Rindler space-time. Therefore, the final mixed state of inertial Alice and noninertial Rob,  $\rho_{AR}$ , can be obtained by tracing out region II of the Rindler space-time. The nonseparability of this relativistic reduced state is characterized using the AR  $q$ -conditional entropy, which takes negative values for nonseparable states and positive values for separable states. We captured the nonseparability of pure multiqubit GHZ and  $W$  states when one of their qubits is accelerated. Further, we studied the nonseparability of mixed states generated by

adding a global noise to the same multiqubit GHZ and  $W$  states when one of their qubits is in uniform acceleration.

The analytical form of the AR  $q$ -conditional entropy for pure multiqubit GHZ and  $W$  states was evaluated using eigenvalues of the state of inertial Alice and Rob's mode in region I ( $\rho_{A_1A_2\cdots A_{N-1}R}$ ) and Rob's subsystem ( $\rho_R$ ). We then numerically studied the nonseparability using the eigenvalue truncation procedure (see Sec. IV A) performed on these infinite-dimensional density matrices  $\rho_{A_1A_2\cdots A_{N-1}R}$  and  $\rho_R$  to get their required nonzero eigenvalues, respectively. The AR  $q$ -conditional entropy  $S_q(A_1A_2\cdots A_{N-1}|R)$  in the inertial-noninertial bipartition always remains less than zero for both pure multiqubit GHZ and  $W$  states with one of their qubits under uniform acceleration, implying that they remain nonseparable for any values of their state parameters and acceleration  $\lambda$ . We observed that irrespective of the value of  $q$ , the nonseparability of  $\rho_{A_1A_2\cdots A_{N-1}R}$  will be high at low values of acceleration and decreases with the increase in acceleration; in particular, the AR  $q$ -conditional entropy  $S_q(A_1A_2\cdots A_{N-1}|R)$  tends to 0 as  $\lambda \rightarrow 1$ . The nonseparability of both the pure multiqubit GHZ and  $W$  states with one of their qubits under acceleration became steeper in its approach to zero as the acceleration  $\lambda$  and the parameter  $q$  increased. Further, we observed that the nonseparability of the pure multiqubit GHZ state with one of its qubits in acceleration is not dependent on the  $N$ , i.e., it is independent of the number of qubits in the inertial frame. However, when the number of qubits in the inertial frame of the pure multiqubit  $W$  state with one of its qubits in acceleration is increased, the nonseparability decreases as  $N$  increases.

We further extended our study to various mixed multi-qubit states  $\rho_{A_1A_2\cdots A_{N-1}B}$ , which are generated by mixing a global noise with the pure multiqubit GHZ and  $W$  states. The nonseparability using the AR  $q$ -conditional entropy  $\mathcal{S}_q(A_1A_2\cdots A_{N-1}|R)$  in the inertial-noninertial bipartition was evaluated for these mixed multiqubit states  $\rho_{A_1A_2\cdots A_{N-1}R}$  when one of their qubits is accelerated. For these mixed multi-qubit states, the AR  $q$ -conditional entropy was numerically calculated by employing the density-matrix truncation procedure (see Sec. V A). We observed that there exist regions of both separability and nonseparability of the state  $\rho_{A_1A_2\cdots A_{N-1}R}$  depending on the choices of acceleration  $\lambda$ , mixing parameter  $p$ , and parameter  $q$ . As  $q$  is increased to large values, the transition curve  $\mathcal{S}_q(A_1A_2\cdots A_{N-1}|R) = 0$  becomes saturated with respect to  $\lambda$  and  $p$ . Hence, the strongest condition for separability for these states in terms of the acceleration and mixing parameter was obtained in the asymptotic limit of  $q$  tending to  $\infty$ . These transition points were fitted to the family of curves given by  $(p/b)^x + \lambda^y = 1$ . The separability conditions for all these mixed multiqubit GHZ and  $W$  states when one of their qubits is in uniform acceleration considered in our study were consolidated in Table I. For a mixed  $N$ -qubit GHZ and  $W$  states with one of their qubits accelerated, we observed that the nonseparable region decreases as the number of qubits in the inertial frame increases. The reduction of the nonseparable region, as acceleration  $\lambda$  is increased, is much faster for the  $N$ -qubit mixed  $W$  state  $\rho_{A_1A_2\cdots A_{N-1}R}^W$  than its  $N$ -qubit mixed GHZ counterpart  $\rho_{A_1A_2\cdots A_{N-1}R}^{GHZ}$ , indicating that, in general, GHZ states can sustain the nonseparability better

than  $W$  states when one of its qubit is uniformly accelerated with respect to the others.

A comparison was made between the nonseparability derived from AR  $q$ -conditional entropy and the entanglement measure logarithmic negativity. In single-qubit-accelerated  $N$ -qubit pure and mixed GHZ and  $W$  states, the nonseparability and entanglement decrease with increasing acceleration, eventually reaching zero in the infinite-acceleration limit. Moreover, the nonseparability and entanglement in the single-qubit-accelerated pure and mixed GHZ states consistently surpass the corresponding  $W$  states for all ranges of acceleration and mixing parameters. Furthermore, in single-qubit-accelerated  $N$ -qubit mixed GHZ and  $W$  states, we observed that the transition from entanglement or nonseparability to separability occurs at different mixing parameter values at different accelerations. For  $N = 2$ , the transition curves for logarithmic negativity and AR  $q$ -conditional entropy are equivalent. However, as  $N$  increases, AR  $q$ -conditional entropy imposes stricter conditions for nonseparability than the logarithmic negativity.

Note that this study can be extended to a fermionic system when one of its qubits is in acceleration; however, this warrants a separate investigation. We believe that our study of nonseparability in various multiqubit states with their subsystem under acceleration will pave the way for exploring numerous information-theoretic physical quantities in relativistic scenarios. This in turn would help in understanding the effect of relativity on quantum systems used in space-based technology or other areas of research where relativity and quantum mechanics are considered together [73,74].

This study also may play a pivotal role in realizing various quantum information protocols where relativistic effects cannot be neglected.

## ACKNOWLEDGMENTS

We acknowledge helpful discussions with P. Kiran. R.P. and H.S.H. acknowledge financial support from the Science and Engineering Research Board, Government of India, under Grant No. CRG/2021/008795. The authors acknowledge that the computations were performed using the High-Performance Computing facility AnantGanak at IIT Dharwad.

## APPENDIX

### 1. Mixed three-qubit GHZ state

A mixed three-qubit GHZ state, with the first two qubits with Alice and the third qubit in Bob's possession, is given by

$$\varrho_{A_1A_2B} = \frac{p}{8} \mathbb{I}_d + (1-p) |\psi_{A_1A_2B}\rangle \langle \psi_{A_1A_2B}|, \quad (\text{A1})$$

where  $|\psi_{A_1A_2B}\rangle = (1/\sqrt{2})(|000\rangle + |111\rangle)$ ,  $\mathbb{I}_d$  is the  $2^3 \times 2^3$  identity matrix, and  $p$  is the mixing parameter. Let us consider that Bob is now uniformly accelerating with respect to Alice and the resulting state, denoted by  $\varrho_{A_1A_2R_I}^{\text{GHZ}_3}$ , is obtained by using the transformations from Minkowski to Rindler space-time in Eqs. (1) and (2). Then the mixed state  $\varrho_{A_1A_2R}^{\text{GHZ}_3}$  after tracing out one of the disjoint regions in Rindler space-time (region II) is given by

$$\begin{aligned} \varrho_{A_1A_2R}^{\text{GHZ}_3} = & \frac{1}{\cosh^2 r} \sum_{n=0}^{\infty} \tanh^{2n} r \left[ \frac{4-3p}{8} \left( |00n\rangle \langle 00n| + \frac{n+1}{\cosh^2 r} |11n+1\rangle \langle 11n+1| \right) \right. \\ & + \frac{1-p}{2} \frac{\sqrt{n+1}}{\cosh r} (|00n\rangle \langle 11n+1| + |11n+1\rangle \langle 00n|) + \frac{p}{8} \left( |11n\rangle \langle 11n| + |10n\rangle \langle 10n| + |01n\rangle \langle 01n| \right. \\ & \left. \left. + \frac{n+1}{\cosh^2 r} (|00n+1\rangle \langle 00n+1| + |01n+1\rangle \langle 01n+1| + |10n+1\rangle \langle 10n+1|) \right) \right]. \quad (\text{A2}) \end{aligned}$$

### 2. Mixed three-qubit $W$ state

A mixed three-qubit inertial state, shared between Alice and Bob, is given by

$$\varrho_{A_1A_2B}^{W_3} = \frac{p}{8} \mathbb{I}_d + (1-p) |\psi_{A_1A_2B}\rangle \langle \psi_{A_1A_2B}|, \quad (\text{A3})$$

where  $|\psi_{A_1A_2B}\rangle = (1/\sqrt{3})(|001\rangle + |010\rangle + |100\rangle)$ ,  $\mathbb{I}_d$  is the  $2^3 \times 2^3$  identity matrix, and  $p$  is the mixing parameter. We consider that Bob is now uniformly accelerating with respect to Alice and the resulting state  $\varrho_{A_1A_2R}^{W_3}$ , after tracing out Rob's modes in region II of Rindler space-time, is given by

$$\begin{aligned} \varrho_{A_1A_2R}^{W_3} = & \frac{1}{\cosh^2 r} \sum_{n=0}^{\infty} \tanh^{2n} r \left[ \frac{8-5p}{24} \left( |01n\rangle \langle 01n| + |10n\rangle \langle 10n| + \frac{n+1}{\cosh^2 r} |00n+1\rangle \langle 00n+1| \right) \right. \\ & + \frac{p}{8} \left( |11n\rangle \langle 11n| + |10n\rangle \langle 10n| + \frac{n+1}{\cosh^2 r} (|00n+1\rangle \langle 00n+1| + |01n+1\rangle \langle 01n+1| + |10n+1\rangle \langle 10n+1|) \right) \\ & + \frac{1-p}{3} \left( |01n\rangle \langle 10n| + |10n\rangle \langle 01n| + \frac{\sqrt{n+1}}{\cosh r} (|01n\rangle \langle 00n+1| + |00n+1\rangle \langle 01n| + |00n+1\rangle \langle 10n| \right. \\ & \left. + |10n\rangle \langle 00n+1|) \right) \right]. \quad (\text{A4}) \end{aligned}$$

- [1] C. H. Bennett, G. Brassard, C. Crépeau, R. Jozsa, A. Peres, and W. K. Wootters, *Phys. Rev. Lett.* **70**, 1895 (1993).
- [2] S. Pirandola, J. Eisert, C. Weedbrook, A. Furusawa, and S. L. Braunstein, *Nat. Photon.* **9**, 641 (2015).
- [3] X.-M. Hu, Y. Guo, B.-H. Liu, C.-F. Li, and G.-C. Guo, *Nat. Rev. Phys.* **5**, 339 (2023).
- [4] C. H. Bennett and S. J. Wiesner, *Phys. Rev. Lett.* **69**, 2881 (1992).
- [5] C. H. Bennett and G. Brassard, in *Proceedings of IEEE International Conference on Computers, Systems, and Signal Processing, Bangalore, India* (IEEE, New York, 1984), pp. 175–179.
- [6] P. W. Shor and J. Preskill, *Phys. Rev. Lett.* **85**, 441 (2000).
- [7] R. Horodecki, P. Horodecki, M. Horodecki, and K. Horodecki, *Rev. Mod. Phys.* **81**, 865 (2009).
- [8] K. Modi, A. Brodutch, H. Cable, T. Paterek, and V. Vedral, *Rev. Mod. Phys.* **84**, 1655 (2012).
- [9] I. Fuentes-Schuller and R. B. Mann, *Phys. Rev. Lett.* **95**, 120404 (2005).
- [10] D. E. Bruschi, J. Louko, E. Martín-Martínez, A. Dragan, and I. Fuentes, *Phys. Rev. A* **82**, 042332 (2010).
- [11] A. Datta, *Phys. Rev. A* **80**, 052304 (2009).
- [12] E. Martín-Martínez and J. León, *Phys. Rev. A* **81**, 052305 (2010).
- [13] B. Richter and Y. Omar, *Phys. Rev. A* **92**, 022334 (2015).
- [14] E. Martín-Martínez and J. León, *Phys. Rev. A* **81**, 032320 (2010).
- [15] D. E. Bruschi, A. Dragan, I. Fuentes, and J. Louko, *Phys. Rev. D* **86**, 025026 (2012).
- [16] F. Buscemi and P. Bordone, *Phys. Rev. A* **84**, 022303 (2011).
- [17] S. Moradi, *Phys. Rev. A* **79**, 064301 (2009).
- [18] E. Martín-Martínez and I. Fuentes, *Phys. Rev. A* **83**, 052306 (2011).
- [19] W.-C. Qiang, G.-H. Sun, Q. Dong, and S.-H. Dong, *Phys. Rev. A* **98**, 022320 (2018).
- [20] J. León and E. Martín-Martínez, *Phys. Rev. A* **80**, 012314 (2009).
- [21] S. Khan, N. A. Khan, and M. Khan, *Commun. Theor. Phys.* **61**, 281 (2014).
- [22] D. Ahn, Y. H. Moon, R. B. Mann, and I. Fuentes-Schuller, *J. High Energy Phys.* **06** (2008) 062.
- [23] D. C. M. Ostapchuk and R. B. Mann, *Phys. Rev. A* **79**, 042333 (2009).
- [24] P. M. Alsing, I. Fuentes-Schuller, R. B. Mann, and T. E. Tessier, *Phys. Rev. A* **74**, 032326 (2006).
- [25] J. Wang and J. Jing, *Phys. Rev. A* **83**, 022314 (2011).
- [26] S. Khan, *Ann. Phys. (NY)* **348**, 270 (2014).
- [27] J. K. Basak, D. Giataganas, S. Mondal, and W.-Y. Wen, *Phys. Rev. D* **108**, 125009 (2023).
- [28] E. Martín-Martínez and J. León, *Phys. Rev. A* **80**, 042318 (2009).
- [29] E. Martín-Martínez, L. J. Garay, and J. León, *Phys. Rev. D* **82**, 064028 (2010).
- [30] X.-H. Ge and S. P. Kim, *Class. Quantum Grav.* **25**, 075011 (2008).
- [31] Q. Pan and J. Jing, *Phys. Rev. D* **78**, 065015 (2008).
- [32] S. Bhattacharya and N. Joshi, *Phys. Rev. D* **105**, 065007 (2022).
- [33] E. Martín-Martínez, L. J. Garay, and J. León, *Phys. Rev. D* **82**, 064006 (2010).
- [34] J. L. Ball, I. Fuentes-Schuller, and F. P. Schuller, *Phys. Lett. A* **359**, 550 (2006).
- [35] I. Fuentes, R. B. Mann, E. Martín-Martínez, and S. Moradi, *Phys. Rev. D* **82**, 045030 (2010).
- [36] G. Ver Steeg and N. C. Menicucci, *Phys. Rev. D* **79**, 044027 (2009).
- [37] S.-M. Wu, H.-S. Zeng, and T. Liu, *Class. Quantum Grav.* **39**, 135016 (2022).
- [38] N. Liu, J. Goold, I. Fuentes, V. Vedral, K. Modi, and D. E. Bruschi, *Class. Quantum Grav.* **33**, 035003 (2016).
- [39] Z. Tian, J. Wang, H. Fan, and J. Jing, *Sci. Rep.* **5**, 7946 (2015).
- [40] M. Ahmadi, D. E. Bruschi, C. Sabín, G. Adesso, and I. Fuentes, *Sci. Rep.* **4**, 4996 (2014).
- [41] M. Ahmadi, D. E. Bruschi, and I. Fuentes, *Phys. Rev. D* **89**, 065028 (2014).
- [42] J. Wang, Z. Tian, J. Jing, and H. Fan, *Sci. Rep.* **4**, 7195 (2014).
- [43] J. Wang, J. Deng, and J. Jing, *Phys. Rev. A* **81**, 052120 (2010).
- [44] P. M. Alsing and G. J. Milburn, *Phys. Rev. Lett.* **91**, 180404 (2003).
- [45] E. Tjoa, *Phys. Rev. A* **106**, 032432 (2022).
- [46] P. T. Grochowski, G. Rajchel, F. Kiałka, and A. Dragan, *Phys. Rev. D* **95**, 105005 (2017).
- [47] S. Khan and N. A. Khan, *Eur. Phys. J. Plus* **130**, 216 (2015).
- [48] S. Haseli, *Eur. Phys. J. C* **79**, 616 (2019).
- [49] N. A. Khan, M. Jan, M. Shah, and D. Khan, *Ann. Phys. (NY)* **440**, 168831 (2022).
- [50] O. Gühne and M. Lewenstein, *Phys. Rev. A* **70**, 022316 (2004).
- [51] V. Giovannetti, *Phys. Rev. A* **70**, 012102 (2004).
- [52] N. J. Cerf and C. Adami, *Phys. Rev. Lett.* **79**, 5194 (1997).
- [53] R. Horodecki and P. Horodecki, *Phys. Lett. A* **194**, 147 (1994).
- [54] R. Horodecki and M. Horodecki, *Phys. Rev. A* **54**, 1838 (1996).
- [55] R. Horodecki, P. Horodecki, and M. Horodecki, *Phys. Lett. A* **210**, 377 (1996).
- [56] M. A. Nielsen and J. Kempe, *Phys. Rev. Lett.* **86**, 5184 (2001).
- [57] C. Tsallis, S. Lloyd, and M. Baranger, *Phys. Rev. A* **63**, 042104 (2001).
- [58] S. Abe, *Phys. Rev. A* **65**, 052323 (2002).
- [59] R. Rossignoli, N. Canosa, and L. Ciliberti, *J. Russ. Laser Res.* **32**, 467 (2011).
- [60] J. Batle, A. R. Plastino, M. Casas, and A. Plastino, *J. Phys. A: Math. Gen.* **35**, 10311 (2002).
- [61] J. Batle, A. Plastino, M. Casas, and A. Plastino, *Eur. Phys. J. B* **35**, 391 (2003).
- [62] C. Tsallis, *J. Stat. Phys.* **52**, 479 (1988).
- [63] C. Tsallis, R. Mendes, and A. R. Plastino, *Physica A* **261**, 534 (1998).
- [64] A. Wehrl, *Rev. Mod. Phys.* **50**, 221 (1978).
- [65] S. Abe and A. K. Rajagopal, *Physica A* **289**, 157 (2001).
- [66] S. Abe and A. K. Rajagopal, *Chaos Soliton. Fract.* **13**, 431 (2002).
- [67] R. Prabhu, A. R. Usha Devi, and G. Padmanabha, *Phys. Rev. A* **76**, 042337 (2007).
- [68] K. G. H. Vollbrecht and M. M. Wolf, *J. Math. Phys.* **43**, 4299 (2002).
- [69] Sudha, A. R. Usha Devi, and A. K. Rajagopal, *Phys. Rev. A* **81**, 024303 (2010).

- [70] C. H. Bennett, G. Brassard, S. Popescu, B. Schumacher, J. A. Smolin, and W. K. Wootters, *Phys. Rev. Lett.* **76**, 722 (1996).
- [71] M. B. Plenio, *Phys. Rev. Lett.* **95**, 090503 (2005).
- [72] A. Peres, *Phys. Rev. Lett.* **77**, 1413 (1996).
- [73] R. Ursin, T. Jennewein, J. Kofler, J. M. Perdignes, L. Cacciapuoti, C. J. de Matos, M. Aspelmeyer, A. Valencia, T. Scheidl, A. Acin *et al.*, *Europhys. News* **40**, 26 (2009).
- [74] S. Schiller, A. Görlitz, A. Nevsky, S. Alighanbari, S. Vasilyev, C. Abou-Jaoudeh, G. Mura, T. Franzen, U. Sterr, S. Falke *et al.*, in *Proceedings of the 2012 European Frequency and Time Forum, Gothenburg, 2012* (IEEE, Piscataway, 2012), pp. 412–418.